AIR FORCE INSTITUTE OF TECHNOLOGY

AIR UNIVERSITY
UNITED STATES AIR FORCE

STUDY OF THE CHARACTERISTICS OF HIGH PRESSURE PROPORTIONAL COUNTERS FOR THE DETECTION OF RADIOACTIVE NOBLE GASES

THESIS

AFIT/GNE/PH/83M-8 Jeffrey J. Knapp
Capt USA

SCHOOL OF ENGINEERING

WRIGHT-PATTERSON AIR FORCE BASE, OHIO

DISCLAIMER NOTICE

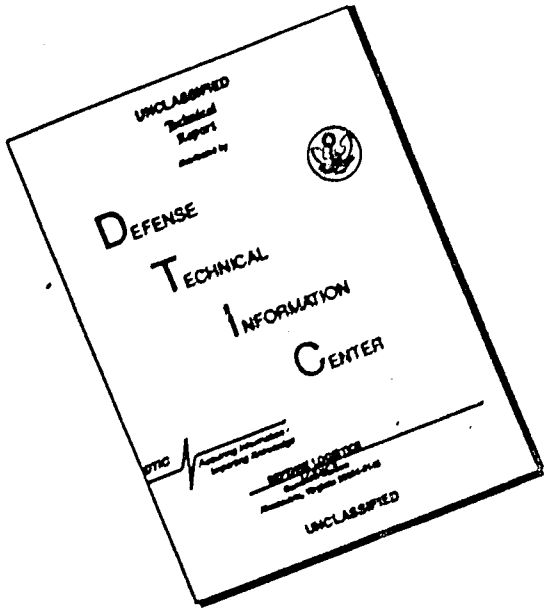

THIS DOCUMENT IS BEST QUALITY AVAILABLE. THE COPY FURNISHED TO DTIC CONTAINED A SIGNIFICANT NUMBER OF PAGES WHICH DO NOT REPRODUCE LEGIBLY.

AFIT/GNE/PH/83M-8

STUDY OF THE CHARACTERISTICS OF HIGH PRESSURE PROPORTIONAL COUNTERS FOR THE DETECTION OF RADIOACTIVE NOBLE GASES

THESIS

AFIT/GNE/PH/83M-8 Jeffrey J. Knapp
Capt USA

Approved for public release; distribution unlimited

AFIT/GNE/PH/83M-8

STUDY OF THE CHARACTERISTICS OF HIGH PRESSURE PROPORTIONAL COUNTERS FOR THE DETECTION OF RADIOACTIVE NOBLE GASES

THESIS

Presented to the Faculty of the School of Engineering
of the Air Force Institute of Technology
Air University
in Partial Fulfillment of the
Requirements for the Degree of
Master of Science

by

Jeffrey J. Knapp, BS, MSSM
Capt USA
Graduate Nuclear Engineering

March 1983

Preface

This thesis was an attempt to portray six months of effort in the development of a new detection system. The endeavor involved the creation of new equipment and techniques to support the effort.

There are too many people to whom I owe thanks to list here. But, to my thesis advisor, Dr. George John, I owe my first debt, the chance to do this work and all the help and suggestions offered by him; he certainly is the most dedicated and hardest working instructor I have ever had. To the technicians in the Physics Department, for their continuous assistance, I am very grateful. To Mr. Short and the personnel of the school shop, I have never worked with a more competent and professional group of people. I am truly indebted not only for their superlative support but also for their friendship.

Finally, I owe the most to my wife Karen and my dog Shiloh, whose patience and support during the entire period really made all this possible.

Jeffrey J. Knapp

Contents

List of Figures

List of Tables

Abstract

This report presents a study of the design and operating characteristics of high pressure proportional counters for the detection of radioactive noble gases. The analysis was limited to those radioisotopes of xenon, ^{131m}Xe and ^{133}Xe, which are produced in nuclear fission. The detector may be utilized for the identification of the radionuclide ^{133}Xe through conversion electron analysis. A sample of ^{133}Xe was measured at 41 atmospheres using xenon as the counting gas; the resolution (FWHM) for the 45 keV conversion electron and 75.6 keV sum peak were found to be 5.9 keV and 7.0 keV respectively. The extreme sensitivity of noble gases to electronegative impurities was also found; a periodic or perhaps continuous purification of the counting gas may be required for stable and reproducible resolution. Recommendations were made for further study.

STUDY OF THE CHARACTERISTICS OF HIGH PRESSURE PROPORTIONAL COUNTERS FOR THE DETECTION OF RADIOACTIVE NOBLE GASES

I. Introduction

Problem

An efficient radiation detector must be developed to measure noble gas radioactive isotopes. The radioactive isotopes of the noble gases provide unique geophysical and meteorological information concerning the properties and history of the atmospheric environment. Radioactive noble gases are produced in significant quantities by nuclear reactors, and reactor fuel processing plants. The release of these radioactive gaseous effluents constitutes a potentially significant impact on the health and welfare of the general populace. Various environmental studies require that selected radioactive isotopes of xenon at low concentrations be measured from atmospheric samples. The measurement of the rare gas radionuclides in our environment provides both an opportunity and a challenge. The opportunity arises from the specific information which such nuclides can reveal concerning current and prior world-wide nuclear processes, whereas the challenge is a result of the extremely low levels of radioactivity with which one must contend. The extremely low activity levels require very special methods of measurement,

systems design, and data interpretation (Ref 1).

This report presents a study of the potential of a high pressure xenon proportional counter for the analysis of radioactive noble gases. The objectives of the study are to design, construct, and test a high pressure proportional counter, and to examine the dependence of the response to voltage and pressure. The utility of the detector in analyzing radionuclides of xenon will be determined. This study was limited to two radioisotopes of xenon, ^{133}Xe and ^{131m}Xe, which are produced in nuclear fission, and to the use of stable xenon as the counting medium.

Background

The analysis of ^{131m}Xe and ^{133}Xe with various detection systems has been a continuing study locally. Rowe (Ref 2) explored the capabilities of a cooled, lithium drifted silicon (Si(Li)) detector to measure ^{131m}Xe radiations. Hunt (Ref 3) and Andrews (Ref 4) each later utilized the same detection system in attempting to quantify a small amount of ^{131m}Xe in the presence of a substantially larger amount of ^{133}Xe. Berggren (Ref 5) studied the utility of a cryogenic argon ionization chamber detector for analyzing quantitatively mixtures of ^{131m}Xe and ^{133}Xe. Benedetti is presently continuing this effort using a cryogenic xenon ionization chamber detector which utilizes a Frisch grid (Ref 6).

Several methods have been employed by others to measure the levels of xenon isotopes in [illegible]

analysis of samples is accomplished by Geiger counting in a small ($\sim$23cm^3) detector with a thin copper wall, inside a NaI (Tl) or Ge well detector, or by toluene-based liquid scintillation counting. Coincidence events occurring in the Geiger-Mueller tube and NaI (Tl) counter at an energy of 81 keV signify that a ^{133}Xe state has been detected; the probability for this gamma-ray is 0.37. By utilizing a 100% efficient gamma-ray detector for 81 keV gamma-rays, 37% of the ^{133}Xe decays can be recorded and identified specifically as ^{133}Xe by coincidence counting. The remainder (63 percent) of the decays are counted together with those of other electron emitting isotopes, but can not be distinguished from them. The overall efficiency for measuring ^{133}Xe in an atmospheric sample is 0.173 (Ref 22:6). NaI (Tl) or Ge counting can detect part of the ^{133m}Xe decays, though at 100% efficiency for the 233 keV gamma-ray of ^{133m}Xe, only 14 percent of the decays would be measured. The remainder, 86 percent of the decays, will be counted in the Geiger counter together with the other electron-emitting isotopes but can not be distinguished from them in a single counting period. Similarly, the 164 keV gamma-ray photons of ^{131m}Xe could be used, but only 2 percent of the decays will be measured.

Horrocks and Studier were the first to demonstrate that it was possible to measure radioactive noble gases in liquid scintillation systems (Ref 7). After an atmospheric sample is taken, the gas chromatographic separations for xenon and krypton are made, and the noble gases are measured by sorbing them

separately into a toluene based scintillation cocktail purged of air. Since the xenon gas is dissolved in the organic liquid of the scintillator, the detection efficiency for electrons approaches 100 percent. In the liquid scintillation counter, the beta continuum of ^{133}Xe is detected, and the conversion electron-emitting-isomers are resolved by repeated counting over a sufficiently long time interval. The data are used in decay analysis of the isotopes. If high levels of ^{133}Xe are found, the scintillation vials are placed in a gamma counter, and the gamma-rays are utilized to measure the mixed radioactive isotopes. The intrinsic efficiency for electromagnetic radiation, however, is very low. For example, 94 percent of 30 keV xenon K-shell x-rays would escape detection through 1 g/cm^2 of liquid scintillator because of the small mass absorption coefficient (0.05 cm^2/g) of the organic reagents (Ref 3:2).

The principal reasons for investigating the use of high pressure proportional counters for the analysis of radioactive noble gases are their theoretically superior resolution compared to a liquid scintillation detector and greater intrinsic efficiency for electromagnetic radiation. For example, the photoelectric mass absorption coefficients of silicon and xenon are 1.17 cm^2/gm and 7.82 cm^2/gm respectively for 30 keV x-rays, compared with 0.05 cm^2/gm for a liquid scintillator. Thus the intrinsic efficiency of a xenon high pressure proportional counter can be over 150 times that of a liquid scintillator and almost 7 times that of a Si semiconductor detector

of the same thickness for the characteristic x-rays of xenon. Consequently, a high pressure proportional counter can offer the electron detection efficiencies of the scintillation detector, and a higher efficiency for the x-rays. Self absorption and geometry problems are eliminated as as with the scintillation and cryogenic ionization chamber detectors, since the radioactive xenon sample is mixed into the detector's medium. In the semiconductor detector, however, the use of a beryllium window and the position and thickness of the solidified xenon create window absorption, detection geometry, and self absorption problems not found in the other detectors (Ref 5).

In the absence of electronic noise, the contribution of the detector to the full width at half maximum (FWHM) of a peak in a pulse-height spectrum can be expressed as

$$\text{FWHM detector} = 2.35\sqrt{EWF} \qquad 1$$

where E is the energy of the emissions corresponding to the peak, W is the average energy required for the creation of one electron-ion pair, and F is the Fano factor (Ref 8:201). Table I contains a comparison of the FWHM contributions of four detectors. The Fano factor listed in the table for liquid argon was not measured experimentally but was calculated from theory (Ref 5:5).

Table I. Comparison of Detector Contributions to Resolution (Ref 5:5)

Detector	W (eV/ ion-pair)	Fano Factor	Limiting Resolution $\sqrt{WF}$	FWHM at 160keV (keV)
Scintillation	179	1.0	13.4	12.58
Silicon	3.62	0.084	0.55	0.52
Liquid Argon	23.6	0.107	1.59	1.49
Xenon Proportional (atmospheric pressure)	21.5	0.17	1.91	1.80

One can immediately see that while the resolution of a xenon proportional counter at atmospheric pressure is not quite as good as a semiconductor or cryogenic argon detector, it is still seven times smaller than for liquid scintillators. If a xenon proportional counter can be operated at sufficiently high pressure without significant degradation of resolution, it would have a higher efficiency and better resolution than liquid scintillators currently used.

High pressure proportional counting has the advantage of being a simple standard method. Proportional counters have been powerful tools for the detection of nuclear and atomic radiations for more than 30 years. If the intensity of low energy radiation must be determined, the proportional counter is still the most suitable counter. For good electron spectral measurements, all electrons must be stopped in a medium, and the deposited energy measured. Since the major problem in

gas counting is the large electron range in an atmospheric counter, the utilization of high pressure would confine the particles within the gas volume. For example, the range in cm required to stop a 160 keV electron in xenon at atmospheric pressure is 10.75 cm, while at a pressure of 50 atmospheres the range is 0.21 cm. In a proportional counter of radius 2 cm, at this pressure and for an energy of 160 keV, only 7.6% of the decays will not deposit their entire energy in the counter. A 160 keV electron is approximately the maximum conversion electron characteristic radiation in ^{131m}Xe and ^{133}Xe, and also exceeds the average beta energy (≈100 keV) in ^{133}Xe. At a pressure of 50 atm, a detector radius of 7cm is required to contain the maximum beta energy (≈346 keV) in ^{133}Xe. Furthermore, at 50 atm pressure, 92% of the 30 keV x-rays are absorbed after traveling 1 cm, compared with 5% at atmospheric pressure. Since in a proportional counter the initial electrons from the ion-pairs formed are multiplied 10^5 to 10^6 times by acceleration in the detector field, a high pressure proportional counter would be ideal to measure the conversion electron decays of xenon isotopes.

Gas proportional counters have already been developed which can operate at high pressure. Legrand et al. (Ref 9) and Baerg (Ref 10) utilized a high pressure 4π proportional counter for measurements of internal conversion electrons. For ^{109}Cd at a pressure of 40 atm., they observed resolutions (FWHM/E) of 28% for the 22keV electron, and 13% for the 88 keV electron; these are 6.16 keV and 11.4 keV respectively (ref

9). Schell developed a low background counter which operated at 8000 torr (~11.5 atm.) to measure ^{14}C, ^{3}H, $^{37,39}Ar$, and ^{81}Kr in atmospheric samples (Ref 11). He found the resolution (FWHM) for 2.9 keV x-rays of ^{37}Ar to be approximately 25 percent of the energy or about 0.73 keV at 10 atm. (Ref 11). High pressure proportional counters were also developed by Batchelor (Ref 12), Gilmer (Ref 13), Costa et al. (Ref 14), Bamberger (Ref 15), and Oeschger (Ref 16).

In summary, high pressure proportional counters can be used to analyze the radioisotopes of xenon, and the spectra can be resolved into a beta continuum, conversion electron and sum peaks. Electron collection efficiency will be very high; x-rays will only have a moderate efficiency. The 30 keV x-rays interacting with xenon at 50 atm. pressure will create ionization which can move counts from the e_k peak to a total energy peak. The utility of a high pressure proportional counter in analyzing radionuclides of xenon needs to be determined.

Approach and Presentation

This study initially required a thorough literature search concerning the use and theory of high pressure proportional counting. Next the first proportional counter and the gas handling system were designed, fabricated, tested, and modified as necessary. The second detector was designed and constructed to correct problems encountered with the first. The operation of the detection system was then examined using

P-10, and argon gas at atmospheric and high pressure (~50 atm.) using exterior gamma sources. Finally, the detector was studied at high pressure (~41 atm.) using xenon gas without quench, mixed with radioactive ^{133}Xe.

The sequence of presentation is as follows. In Chapter II, information concerning the noble gas of interest, xenon, is presented. Chapter III covers the theory of proportional counting. Chapter IV contains the design and construction of the two detectors, and the gas handling system. Chapter V presents the operating procedures, the characteristics of each detector, and the results obtained. Finally, the conclusions and recommendations for further work are presented in Chapter VI.

II. Characteristics of the Noble Gas Sample

Introduction

This chapter presents the production and nuclear decay data for ^{131m}Xe and ^{133}Xe. In addition, methods of radiation analysis and the predicted response of a high pressure proportional counter are presented. This information is used throughout this study and is needed for the assessment of system characteristics.

The element xenon has an atomic number 54 and an atomic weight of 131.30 on the ^{12}C scale. At room temperature xenon is a colorless, odorless, and nontoxic gas. Natural xenon consists of nine stable isotopes whose mass numbers range from 124 through 136 (Ref 17:1106). In addition, 27 radioactive isotopes and isomers have been produced artificially in nuclear reactors and in particle accelerators (Ref 18:29). Xenon is found in nature as a constituent of the atmosphere where it occurs to the extent of 8.6×10^{-6}% by volume of dry air. It is the rarest of the stable elements with an estimated abundance of 2.9×10^{-9}% of the earth's crust. Most of the xenon in nature is of primordial origin, but it has been estimated that about 0.5% of the total results from spontaneous or neutron induced fission of uranium and thorium (Ref 19:79).

Production

Xenon and krypton are the principal noble gases produced by nuclear fission. The gaseous effluents of operating nuclear reactors and spent fuel reprocessing plants contain significant quantities of both stable and radioactive isotopes of these two noble gases. The principal radionuclides available for analysis depends both on the fission yield and time of sampling. Samples are usually analyzed hours or days after production, therefore the nuclides present will be those having the longest half-lives, though possibly not the highest yields. Table II lists the cumulative fission yields for the principal isotopes of xenon from the fissioning of ^{235}U.

Table II. Cumulative Fission Yields for Xenon (Ref 20:69)

Isotope	Half-life	Fission Yield %
131m	12.0 days	0.017
131	stable	2.770
132	stable	4.130
133m	2.26 days	0.190
133	5.27 days	6.770
134	stable	7.190
135m	15.7 minutes	1.050
135	9.20 hours	6.720
136	stable	6.120
137	3.80 minutes	5.940
138	14.2 minutes	6.240
139	40.0 seconds	4.960

The very low value for the fission yield of ^{131m}Xe would seem to indicate that this particular radioisotope does not make a significant contribution to the total activity produced by radioactive noble gas effluents. At early times, this may

Table III. The Effect of Decay Time on the Relative Activity of Radioactive Noble Gas Mixtures from ^{235}U Fission from Thermal Neutrons (Ref 21:76)

		Percent of Total Activity After the Indicated Decay Time			
Isotope	Half-life	2 min.	2 hrs	3 days	60 days
^{139}Xe	41.0 sec	3.0			
^{89}Kr	3.2 min	8.2			
^{137}Xe	3.8 min	11.3			
^{135m}Xe	15.0 min	4.6	0.1		
^{138}Xe	17.0 min	14.1	0.3		
^{87}Kr	1.3 hrs	7.3	5.7		
^{83m}Kr	1.9 hrs	1.3	1.4		
^{88}Kr	2.8 hrs	10.2	13.5		
^{85m}Kr	4.4 hrs	4.2	6.7		
^{135}Xe	9.2 hrs	17.2	32.2	0.5	
^{133m}Xe	2.3 days	0.5	1.0	1.5	
^{133}Xe	5.3 days	18.0	30.0	96.7	2.5
^{131m}Xe	12.0 days	0.1	0.2	0.8	1.0
^{85}Kr	10.7 years	0.1	0.1	0.5	96.5

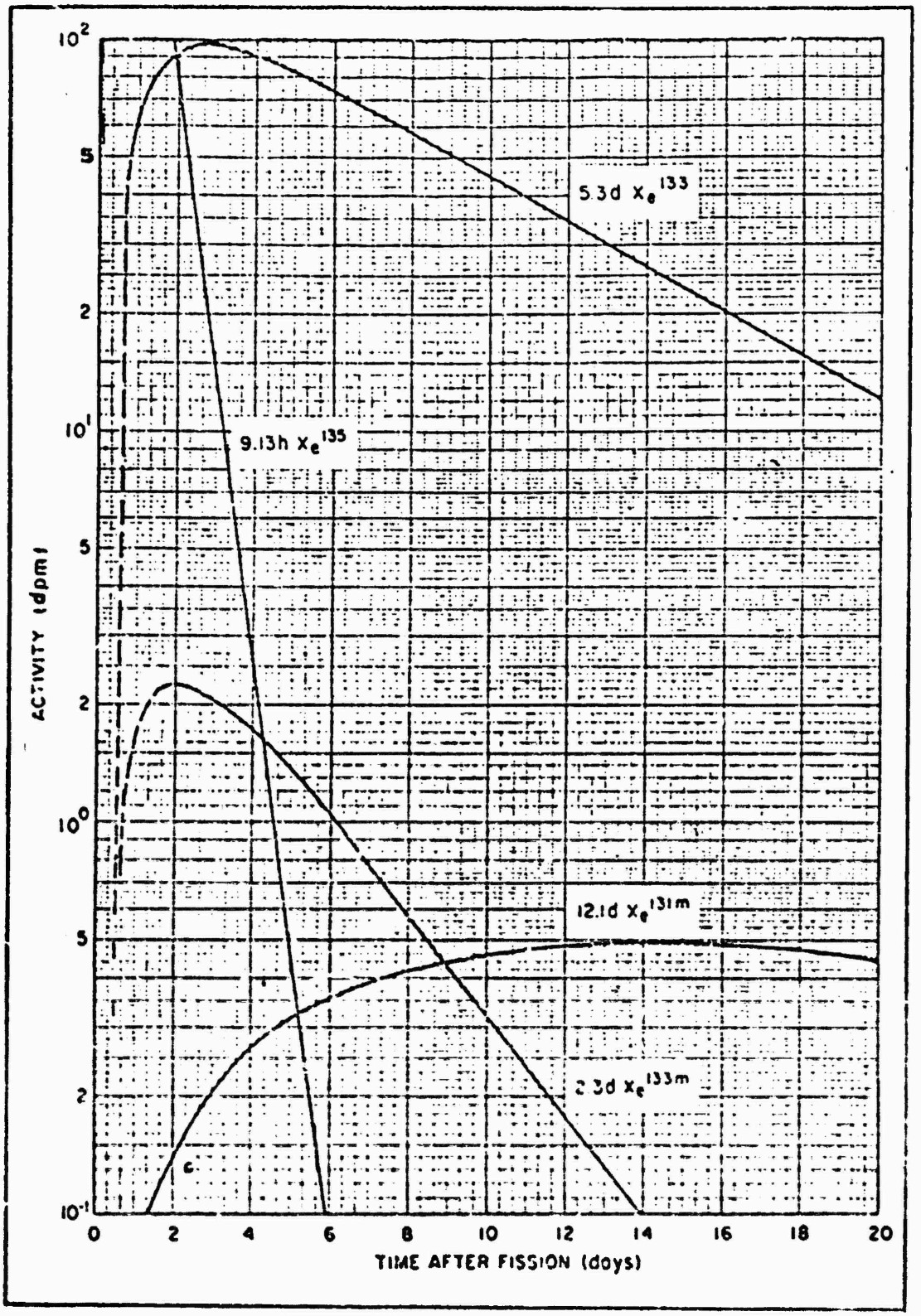

Figure 1. Growth and Decay of Xenon Isotopes in Unfractionated Mixed Fission Products from Thermal Neutron Fission of ^{239}U (Ref 22).

indeed be true. Table III shows, however, that ^{131m}Xe, due to its longer half-life, contributes increasingly to the total activity of the noble gases as the others decay away. Only ^{131m}Xe, ^{133}Xe, and ^{133m}Xe have half-lives reasonably large enough to be considered. Figure 1 shows that ^{135}Xe decays to negligible amounts after 6-8 days, and after only 9 days the concentration of ^{131m}Xe is greater than that of ^{133m}Xe, which decays to negligible amounts in approximately 20 days. After this time, the ^{131m}Xe ($t_{1/2}$ of 12.1 days) and the ^{133}Xe ($t_{1/2}$ of 5.2 days) are the predominant radionuclides present. Thus it was decided to use the radioisotopes ^{131m}Xe and ^{133}Xe in this study. One of the major tasks then is to measure ^{131m}Xe in the presence of about 50 times this amount of ^{133}Xe.

Nuclear Decay Data

The decay scheme for ^{133}Xe is shown in Figure 2. The isotope decays predominantly (99.3%) by beta emission to the first excited state (81 keV) of ^{133}Cs. This state has a moderate internal conversion coefficient (e_k: γ=1.4:1), giving a mixture of gamma rays and internal conversion electrons followed by characteristic cesium K-shell x-rays or Auger electrons. The characteristic radiations and their fractions per decay are listed in Table IV.

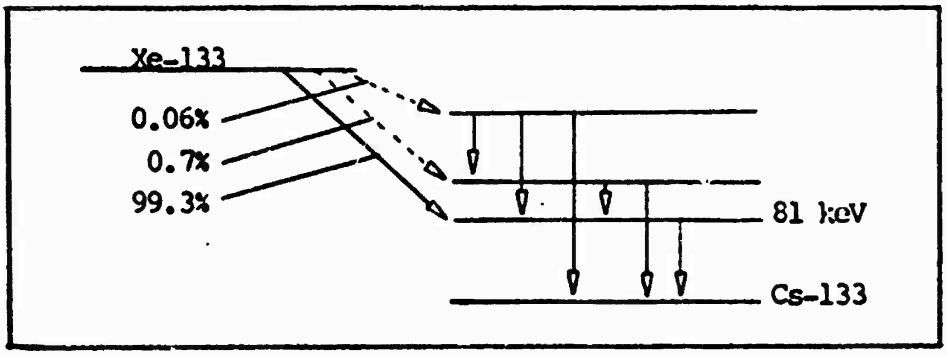

Figure 2. Decay Diagram of ^{133}Xe (Ref 23:279)

Table IV. Characteristic Radiations of ^{133}Xe (Ref 24:387-388)

^{133}Xe B- decay	(5.245 days)		I(min) = 0.10%
Radiation Type	Energy (keV)	Intensity (%)	(g-rad/ μCi-hr)
Auger-L	3.55	49.0 20	0.0037
Auger-K	25.5	5.5 7	0.0030
Ce-K-1	43.636 11	0.30 6	0.0003
Ce-K-2	45.0124 4	52.0 3	0.0498
Ce-L-2	75.2827 4	8.49 20	0.0136
Ce-MNO-2	79.7799 4	2.3 3	0.0039
β^- 1 max	266. 3		
avg	75. 10	0.66 10	0.0011
β^- 2 max	346. 3		
avg	100.5 10	99.34 10	0.213
Total β^- avg	100.3 10	100.01 15	0.214
X-ray L	4.29	6.1 17	0.0006
X-ray $K\alpha_2$	30.6251 3	13.3 3	0.0087
X-ray $K\alpha_1$	30.9728 3	24.6 5	0.0163
X-ray Kβ	35	8.84 20	0.0066
γ_1	79.621 11	0.22 6	0.0004
γ_2	81	37.1 4	0.0640

The decay diagram of ^{131m}Xe is presented in Figure 3. This isotope is an isomeric state of stable ^{131}Xe and is the radioactive progeny of Iodine-131. Xenon-131m has a high internal conversion coefficient (e_k: γ=32:1) and thus, the energy spectrum is dominated by internal conversion electrons, characteristic xenon K-shell x-rays and Auger electrons. The characteristic radiations of ^{131m}Xe are listed in Table V.

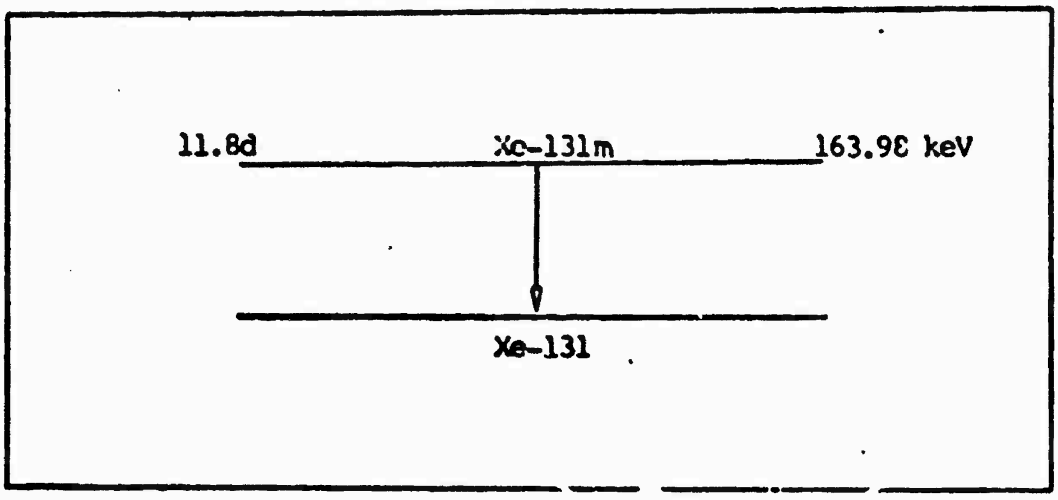

Figure 3. Decay Scheme for ^{131m}Xe (Ref 23:277).

Methods of Radiation Analysis

The results of previous calculations show that the abundance of ^{133}Xe is 50 times that of the $^{131m,133m}Xe$ isotopes. In practical terms, the ^{133m}Xe and ^{131m}Xe isotopes are not presently measureable in normal atmospheric samples (Ref 22:10). The four methods of radiation analysis which could possibly be used to quantify ^{131m}Xe in the presence of

Table V. Characteristic Radiations of ^{131m}Xe (Ref 24:386)

^{131m}Xe (11.9 days)					
Radiation Type	Energy (keV)		Intensity %		(g-rad/ μCi-hr)
Auger-L	3.43		75	4	0.0055
Auger-K	24.6		6.8	13	0.0036
Ce-K-1	129.369	8	61.2	7	0.169
Ce-L-1	158.477	8	28.6	6	0.0965
Ce-M-1	162.788	8	6.50	20	0.0225
Ce-NOP-1	163.722	8	1.78	6	0.0062
X-ray L	4.1		8	3	0.0007
X-ray $K\alpha_2$	29.4580	10	15.5	5	0.009[illegible]
X-ray $K\alpha_1$	29.7790	10	28.7	8	0.0182
X-ray Kβ	33.6		10.2	4	0.0073
γ1	163.93	8	1.96	6	0.0068

^{133}Xe are 1) x-ray spectroscopy, 2) gamma-ray spectroscopy, 3) internal conversion electron analysis, and 4) coincidence analysis techniques.

Since ^{131m}Xe and ^{133}Xe both decay partially by conversion electrons with probabilities of emission of K internal conversion electrons of 61 and 53 percent respectively, one possible method could utilize x-ray counting. The fluorescent yield for the K x-rays is 88.9 percent (Ref 23). X-ray spectroscopy is only possible if the spectral resolution of the detection system is at least 0.5 keV or better to differentiate between the xenon characteristic x-rays emitted in the decay of ^{131m}Xe ($K\alpha_1$ is at 29.78 keV), and the cesium characteristic x-rays

emitted in the decay of ^{133}Xe ($K\alpha_1$ is at 30.97 keV). Xenon - 131m has a very high internal conversion coefficient (e_k: γ=32:1), and emits a gamma ray in only 2% of its decays. Thus gamma ray spectroscopy is not attempted in this study. Analysis of internal conversion electrons, however, was attempted with the high pressure xenon proportional counter. With the electron resolutions already found in high pressure counters (~15-20%), the spectra can be resolved into a beta continuum, conversion electron, and sum peaks. The analysis is, however, complicated by the beta spectrum associated with ^{133}Xe. Coincidence analysis techniques are not attempted in this study; such studies can not be undertaken with a thick-walled high pressure proportional counter having a 4π geometry and intrinsic efficiency of 1.0.

Predicted Response of a High Pressure Proportional Counter

While it was the goal to determine by experiment the capabilities of the detection system used in this project, most results were purely qualitative because of the spectral degradations caused by the equipment. Consequently, it was necessary to postulate a theoretical pulse-height spectrum for the radionuclides ^{131m}Xe and ^{133}Xe, using best estimates of the efficiency and resolution of this detection system.

Basic assumptions for the proportional counter and sample include: 1) 100% detection efficiency for 45 keV electrons, 2) 92% absorption of 30 keV x-rays 1 cm from the counter wall, 3) [illegible] were calculated using equation 1a below, and 4)

degree electron trajectories, 4) a radioactive sample with a ratio of ^{133}Xe to ^{131m}Xe of approximately 50 to 1, 5) summing occurs, 6) photopeaks are assumed to be pure Gaussian curves, 7) internal conversion photopeak resolution is the same as that obtained experimentally for 45 keV electrons, or 5.9 keV (FWHM), 8) a resolution for electromagnetic photopeaks is assumed to be 5.0 keV, obtained theoretically and based on experimental observations, 9) a background of 0.10 CPM/keV is assumed from experimental observations. Edge effects were calculated using the following equation:

$$f_{max} = 1/2[(2rR+R^2)/(r^2)] \qquad 1a$$

where

f_{max} = fraction of decays which do not deposit all of their energy

R = range of electron (cm)

r = radius of detector (cm)

For example, 7.8% of the decays for a 160 keV electron do not deposit all of their energy, and would produce edge effects.

The total activity of the radioactive sample of ^{133}Xe and ^{131m}Xe is 50 disintegrations per second; time of collection is 100 seconds. The profile of the beta continuum was taken from Schell (Ref 22). Branching ratios and characteristic radiations of ^{131m}Xe and ^{133}Xe were taken from Tables IV and V. The predicted spectrum is presented in Figure 4.

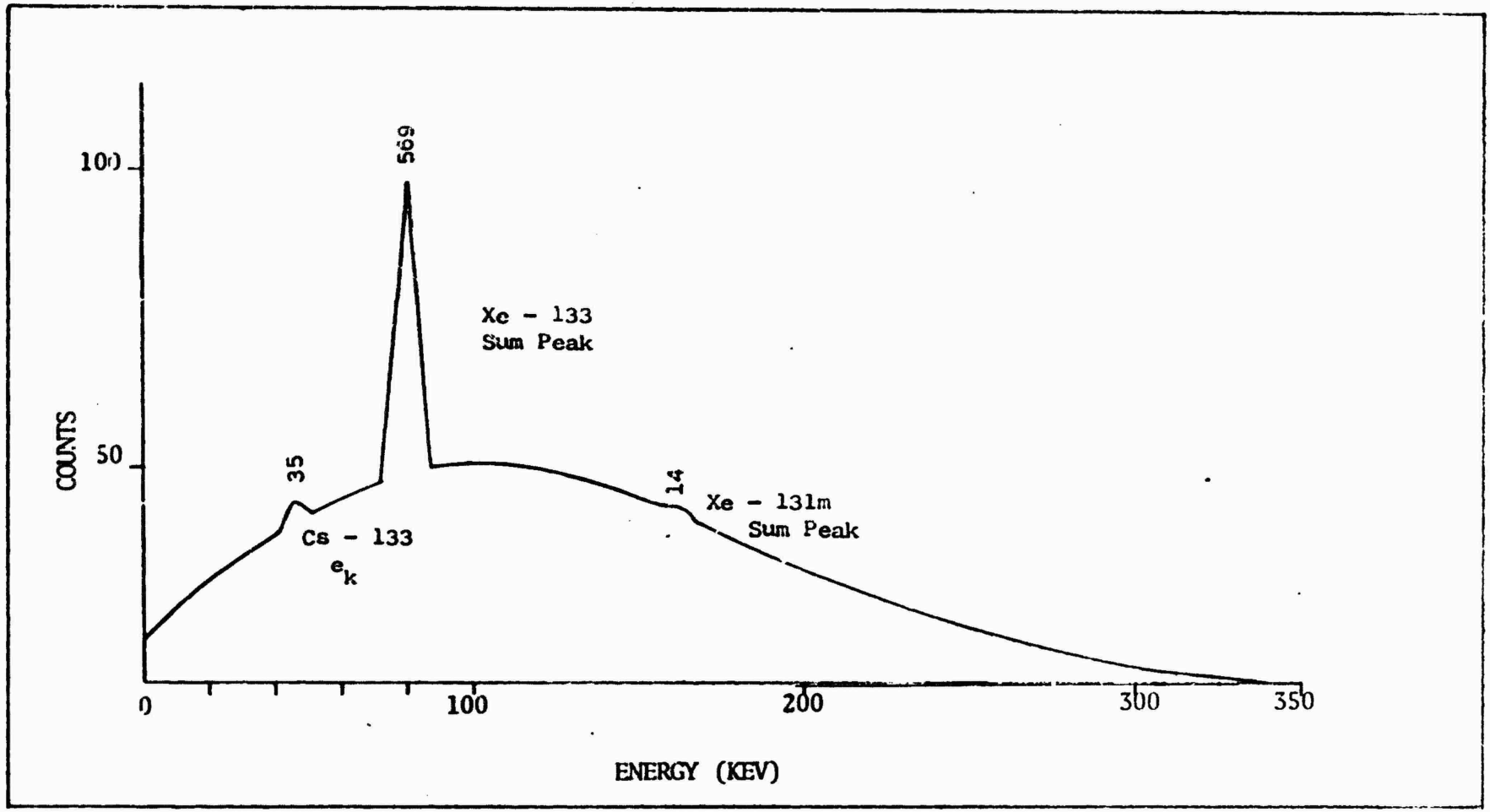

Figure 4. Theoretical Xe-133 and Xe-131m Pulse Height Spectrum With Summing Effects. Secondary (Line) Spectrum 1/10 Scale Size.

III. Theory of Proportional Counting

Introduction

In a proportional counter, the output pulse is proportional to the energy deposited by any event which produces ionization. The electrons from the ionized gas suffer further ionizing collisions on their passage to the anode wire as they are accelerated by the high field near the anode wire. In this manner the pulse height can be increased considerably, by up to 10^5 times, without loss of proportionality. As the voltage is increased, the chamber passes characteristically through the ionization chamber, proportional, limited proportional, and Geiger regions, until eventually breakdown occurs (Ref 25:303). A brief review is given below concerning some parameters and physical effects which influence the mechanism of the high pressure proportional counters designed for this study. The following topics are discussed: gas amplification, positive ion and electron transit times, electron drift velocity, noble gas mixtures, effects of electronegative impurities, end effects, and eccentricity of the wire, space charge effects, resolution, and spurious pulses and afterpulses.

Gas Multiplication

Proportional tubes rely on the phenomenon of gas multiplication to amplify the charge represented by the original

ion pairs created within the gas. Gas multiplication is a consequence of increasing the electric field within the gas above a threshhold value at which secondary ionization will occur. For a cylindrical counter of diameter 2b with the anode wire of diameter 2a, the electrical field strength E per unit pressure at the distance r from the center is given by the relation

$$S(r) = E(r)/p = V/[pr\ln(b/a)] \qquad 2$$

where p is pressure.

Large values of the electric field therefore occur in the immediate vicinity of the anode wire where r is small. Consequently, multiplication of electrons occurs near the anode.

At low values of the field, the electrons and ions created by the incident radiation simply drift to their respective collecting electrodes; positive ions travel slowly to the cathode, and electrons quickly toward the anode. Many collisions normally occur with neutral gas molecules during the migration of these charges. Positive or negative ions achieve very little average energy between collisions due to their low mobility. The electrons, however, are accelerated in the inhomogeneous field towards the central wire, and at a certain distance r_o' from the cylinder axis, ionization of the gas molecules commences. The electrons liberated by this secondary ionization process will also be accelerated by the electric field. The gas multiplication process takes the form of a cascade, the Townsend avalanche, where each free electron

in a collision can potentially create more free electrons by the same process.

If an amount of energy ε is deposited in the counter, then the mean number of ion pairs formed initially is given by $N = \varepsilon/W$, Where W is the mean energy per ion pair. If space charge effects, recombination, photoelectric effects, and electron attachment due to impurities can be neglected, then the mean amplification factor G is given by

$$\ln \bar{G} = - \int_{r_o}^{a} \alpha \, dr \qquad 3$$

where α is the mean number of ion pairs formed by one electron per cm of path (first Townsend coefficient). The reciprocal of α is the mean free path for ionizing collisions. The first Townsend coefficient α/p is a function of E/p and of the nature of the gas. Figure 5 demonstrates this dependence for the rare gases (Ref 26:103).

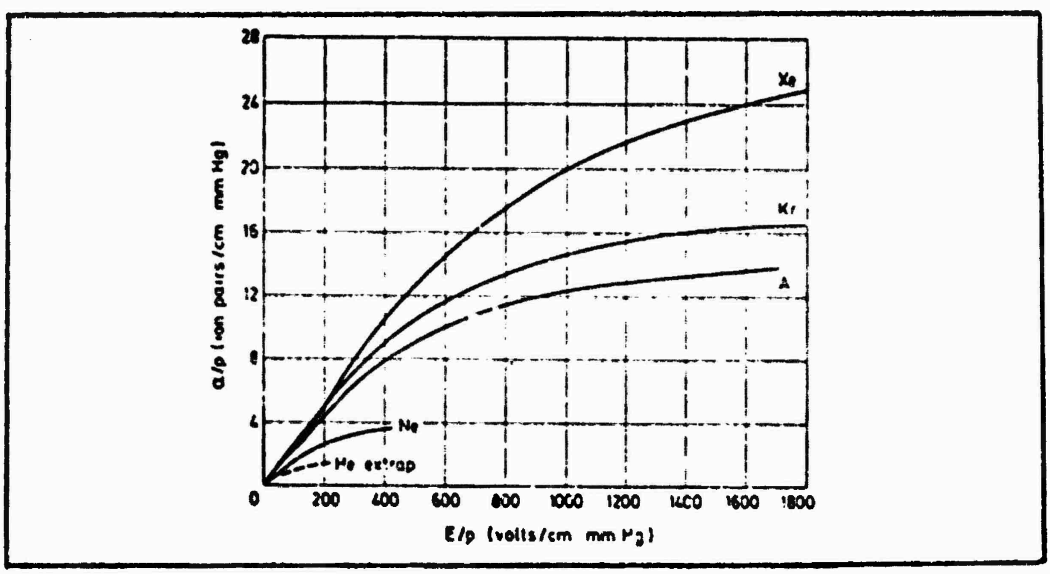

Figure 5. First Townsend Coefficient α/p as a Function of the Electric Field E/p for Rare Gases

The form of the curve depends on the probability of ionization, the electron energy distribution, and electron mobility.

From equations 2 and 3

$$\frac{\ln \bar{G}}{paS(a)} = \int_{S(o')}^{S(a)} \frac{\alpha}{p} \frac{1}{s^2} ds \qquad 4$$

where S(a) and S(o') are the values of S at the anode and at radius r_o, (Ref 26:103).

In principle from knowledge of α and its dependence on electric field strength, the above equation can be integrated to give G in terms of counter parameters. However, since data on α are not extensive, various semi-empirical formulae have been developed to estimate the expected value of gas multiplication, depending on the function used for the first Townsend coefficient, $\alpha/p = f(s)$.

It is usually convenient to use an extrapolated intercept S(o), so that providing S(a) > S(o)

$$\frac{\ln \bar{G}}{paS(a)} = \int_{S(o)}^{S(a)} \frac{\alpha}{p} \frac{1}{s^2} ds \qquad 5$$

or in abbreviated form

$$\psi = K + \frac{S(a)}{S(o)}[\phi] \qquad 6$$

where K is a constant characteristic of the gas, and dependent upon the choice of S(o) (Ref 27:96). Table VI indicates in chronological order the different forms of α/p which have been utilized, and the resulting form of ϕ (Ref 27:97).

Table VI: Forms of α/p and ϕ

Reference	α/p	ϕ
Rose and Korff (Ref 28)/ Curran and Craggs (Ref 29)	$As^{1/2}$	$-2a/s^{1/2}$
Khristov	B	-B/s
Diethorn	CS	C ln S
Williams and Sara (Ref 30)	$Dexp(-E/S)$	$(D/E)exp(-E/S)$
Zastawny (Ref 31)	$F(S-S(o))$	$F(\ln S + S(o)/S)$
Charles	$Jexp(-H/S^{1/2})$	$(2J/H^2)[H/(S^2+1)]\cdot exp(-H/S^{1/2})$

Gas dependent parameters must be deduced from measurements. Zastawny holds that there are five different regions of S with different functional dependences of α/p on S (Ref 31:181). Therefore it depends on the nature of the gas, and the value of S in the counter as to which formula will yield the better results. The use of the formulae of Diethorn, Charles, and Zastawny, with suitably chosen constants, best describes the gain over a range of counter gases and S(a) values.

Positive Ion and Electron Transit Times

The collecting times of electrons and positive ions which are formed in the avalanche near the anode, greatly influences the shape of the formed pulse. The contribution of the electrons to the total pulse is rather small compared to the positive ions, amounting to only a few percent. However the electron transit time is of considerable importance in com-

sidering the maximum counting rate, for example in a 4π counter utilized for beta detection, it represents the maximum rise time of the pulse. This limiting case arises when a beta particle, for example, crosses a cylindrical counter in a plane containing the anode. Primary electrons created at the cathode will make no significant contribution to the pulse until τe seconds later. The electron transit time must be regarded as the effective dead time of a proportional counter in which the particle track length is comparable with counter dimensions, although the counter is not necessarily inoperative at this time (Ref 32:221). The parameter τe can be described by the relation

$$\tau e = aS(a) \int_{S(r)}^{S(a)} dS/[S^2 w_-(S)] \qquad 7$$

where $w_-(S)$ is the drift velocity of the electrons (Ref 26:107). The electron transit time varies rather slowly with pressure, since a change in pressure requires a change in counter potential to maintain the same gas gain (Ref 32:226).

Under conditions in which the electron transit time is long, i.e., in a high pressure counter of fairly large dimensions, there is a danger that spurious pulses will be observed. For minimum transit time of electrons in the counter, it would be advantageous to operate the counter at E/p values where the electron drift velocity is at a maximum. A minimum transit time of electrons between the cathode and anode can be achieved by using a small cathode diameter, and large anode

diameter (Ref 33:364). This proves very difficult in a high pressure proportional counter, for the anode wire must be especially thin to reduce operating voltages.

The transport of positive ions is much slower due to the longer distance, extending practically from the anode to the cathode, and also to the drift velocity $w_+(S)$ which is approximately a thousand times less than electrons. The transit time τ_+ of positive ions can be calculated by a similar relation

$$\tau_+ = aS(a) \int_{S(b)}^{S(r)} dS/[S^2 w_+(S)] \qquad 8$$

(Ref 2f:107).

Electron Drift Velocity

For any gas the drift velocity w is a function of E/p, where E is the applied field strength, and p is the pressure (Ref 34:768). The drift velocity is often expressed in terms of the mean free path between collisions of the charged particles with gas molecules

$$w = \text{const}\ (\lambda/u)(E/p) \qquad 9$$

where λ/p = electron mean free path at the pressure p

u = root-mean-square electron velocity of agitation

μ = mobility = const (λ/u)

Electron drift velocity in the noble gases is extremely sensitive to gaseous impurities. Inelastic collisions between electrons and gas molecules occur only when the electrons have

an energy larger than the first excitation level of the molecule. In argon, for example, the first excitation level is 11.5 eV. In pure argon, even with moderate fields, the electrons will reach a very high agitation energy - of the order of 10 eV. In CO_2, however, inelastic collisions occur very frequently for small electron energies, because of the large number of low excitation levels of the CO_2 molecule. It follows that the addition of a small amount of CO_2 to argon will reduce the average energy of the electrons considerably. Since the drift velocity is directly proportional to the mean free path, and inversely proportional to the square root of the agitation energy, the decrease in the latter quantity caused by the addition of CO_2 to argon will result, in two ways, in an increase of the drift velocity. In fact, the addition of 5-10% CO_2 to argon increases w by as much as ten times for a fixed E/p (Ref 34:784). Lower values of drift velocity can be obtained in a gas of high purity. The conclusion to be drawn is that accurate predictions as to electron behavior cannot be made except for proportional counters containing very pure gases. The drift velocity curve for xenon and argon is presented in Figures 6 and 7. Note in Figure 7 the effect of purification of argon on the electron drift velocity; a reduction in drift velocity, as explained earlier, results.

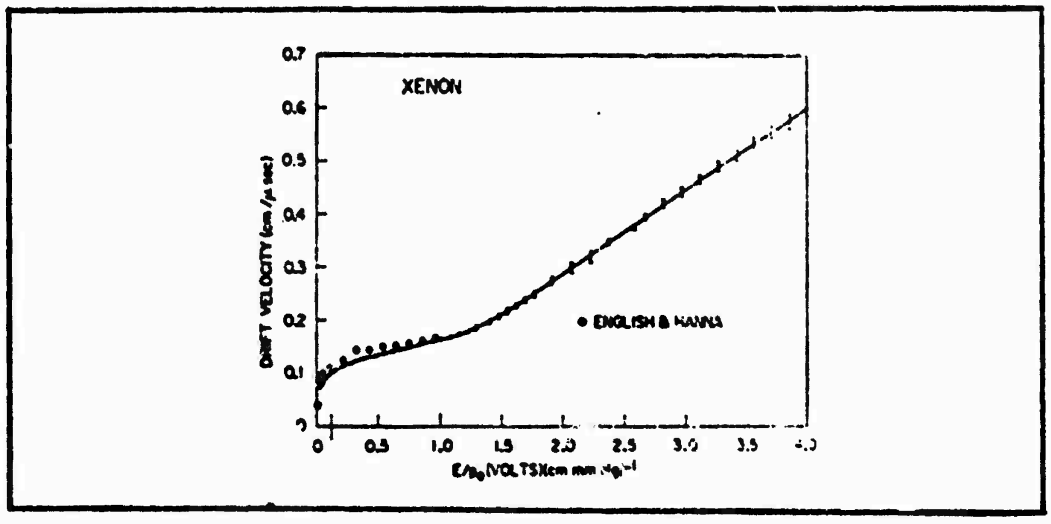

Figure 6. Drift Velocity of Electrons Measured at p = 267 mm Hg (Ref 35:1414).

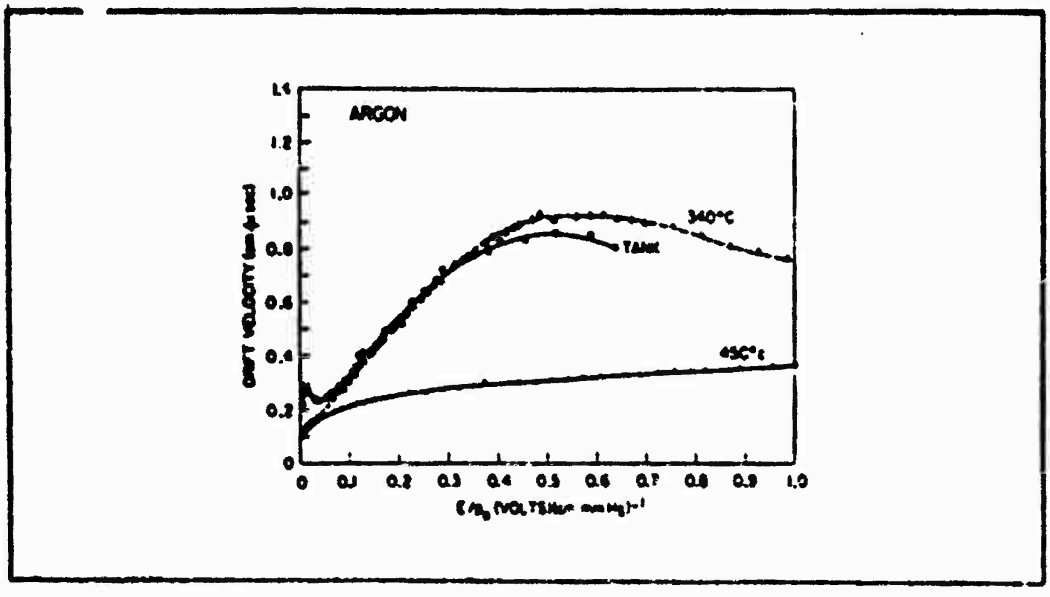

Figure 7. Drift velocity of Electrons Measured at p = 680 mm Hg (Ref 35:1413).

Noble Gas Mixtures

Two fundamental processes take place in the detecting gas 1) primary charge carriers are generated as a result of the

interactions of the ionizing particles, and 2) the multiplication of the charge to a measureable level takes place in a relatively small volume near the anode wire. Because of their small capture cross sections and their good saturation characteristics, mixtures based on the noble gases are the most widely used. Xenon is of practical importance because of its high particle stopping power, and high absorption coefficient for x-rays.

In a proportional counter, since the electrons gain sufficient energy to ionize, they also cause excitation of electronic levels with the subsequent emission of ultraviolet radiation. The emission of photoelectrons at the cathode initiates a new avalanche, and after several repetitions a rapid rise in amplification results. In gases with polyatomic additives, however, over the greatest part of the path of the electrons, their energy is insufficient for electronic excitation in the gas molecules. Most of the inelastic collisions may excite only vibrational and rotational energy, so that except near the wire, only infra-red radiation can be emitted. The energy of the electrons rises more slowly than in the simple gas, and the spatial extent of the ultraviolet region near the wire is considerably smaller. Polyatomic additives quench the emission of the ultraviolet by providing a more probable mode of energy loss for the lower energy electrons, and by failing to contribute to such emission even when the excitation of electronic levels is energetically possible (Ref 28:857).

Noble gases, either in pure or in binary mixtures, can be useful proportional gases provided the gas multiplication factor is kept below 100 (Ref 36:389). Beyond this point, polyatomic additives are required. Operation of a high pressure counter with an anode wire of 10μ diameter and a proportional multiplication factor $\sim 10^2$ are illustrated in Figures 8 and 9.

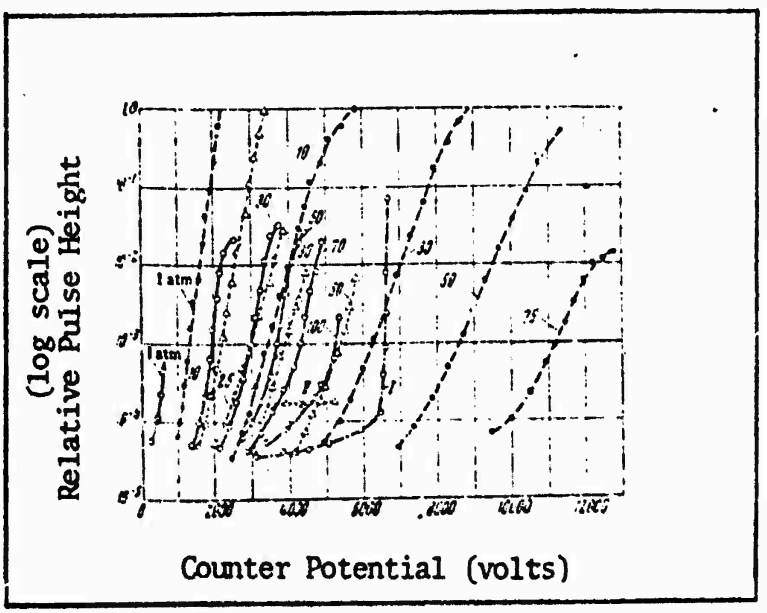

Figure 8. Pulse Height Characteristics of Counter Filled with Gaseous Argon (solid lines), Methane (dashed lines), and Xenon (dot-dash lines). Numbers on the Curves Indicate the Gas Pressure in Atmospheres (Ref 37:829)

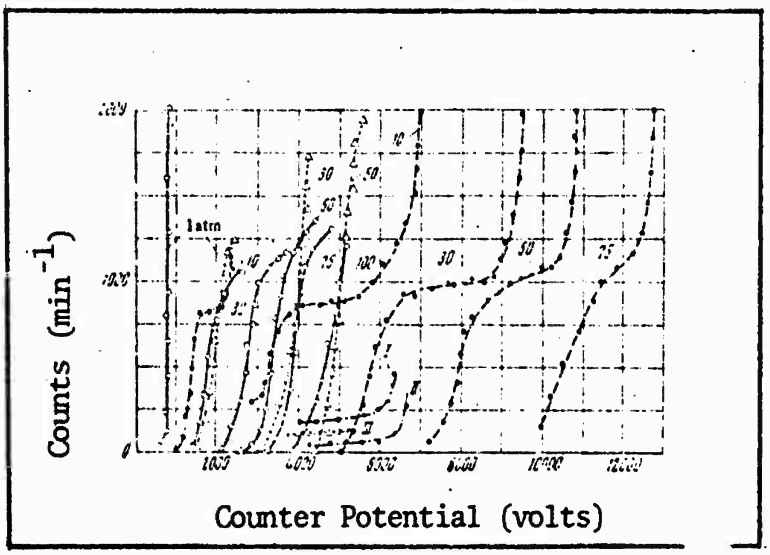

Figure 9. Counting Characteristics of Counter Filled with Gaseous Argon (solid curves), Methane (dashed curves), and Xenon (dot-dash curves) (Ref 37:830).

As shown in Figures 8 and 9, with increasing gas pressure above 50 atm., the pulse height drops appreciably. The counts decrease, and the slope increases. Pisarev et al. found that the operation with pure gases was unstable at high pressures; stable operation was only possible with mixtures of noble gases and polyatomic additives; continuous purification was required for high pressure operation (Ref 37:830).

The ionization yield of a noble gas can be increased remarkably by the addition of a very small quantity of any gas (the Jesse effect) which is interpreted well in terms of the Penning process

$$X^m + Y \rightarrow X + Y^+ + e^- \qquad 10$$

where X^m is a metastable noble gas atom and Y a foreign atom whose ionization potential is lower than the excitation energy of a metastable inert gas atom (Ref 38:1017-1018). This reaction is probably due to the existence of metastable states in the noble gas excitation spectrum, and to the photon resonance absorption by molecules of the main gas. Furthermore, the ionization yield in noble gases increases by the addition of any foreign gas whose ionization potential I_y is higher than the excitation energy E_{xm} of the metastable states of the noble gas. A remarkable difference of this effect from the Jesse effect is that a much larger quantity of the foreign gas is required to make the effect measureable. This observed increase in ionization yield is due to noble gas atoms in non-metastable states which are higher than I_y, and that these states persist long enough to allow collisions of the non-metastable Penning ionization (Ref 38:1018). In a proportional counter, these effects improve the resolution, since the mean ionization energy and the Fano-factor decrease (Ref 36:389). Energies of metastable levels and ionization potentials of the inert gases are shown in Table VII.

Effect of Electronegative Impurities

These impurities result from an admixture of electronegative gases in the gas filling at the beginning of a measurement, or a change in the composition of the gas filling during long-term measurements, possibly caused by the release of various gases adsorbed on the surface and cavities inside the

Table VII. Energies of Metastable Levels and Ionization Potentials of the Inert Gases in eV. (Ref 38:1018).

Element	Metastable Levels				Ionization Potential
	$^3P_2$	^3P_o	^1S_o	$^3S_1$	
He	20.96	20.96	20.62	19.81	24.58
Ne	16.62	16.72			21.56
A	11.53	11.72			15.76
Kr	9.82	10.51			14.00
Xe	8.32	9.41			12.13

counter. The pollutants can decrease the drift velocity of electrons, or if they contain electronegative molecules, they can capture primary electrons. The most dangerous impurities with high electron affinity are halogens, sulphur oxides, water vapors, oxygen, etc. The electronegative impurities easily capture electrons freed by the ionizing particle, and form negative ions (Ref 33:367). Losses of primary electrons caused by attachment processes increase for gases in which the drift velocity of electrons are lower, and as the pressure is increased. Small changes in the concentration of impurities cause shifts in the counting plateau, influences long-term counting stability, and affects the pulse-height distribution.

Recombination

Positive ions accumulating in the detector medium may combine with a drifting electron to form a neutral atom, stop-

ping the electron's contribution to a detected pulse. The probability of recombination is a function of the applied field and the concentration of positive ions in the medium. The recombination of two oppositely charged ions is described in terms of their recombination coefficient β. It is defined as the recombination rate dn/dt per unit volume and unit time divided by the ion densities n^+ and n^-

$$dn/dt = \beta n^+ n^- \qquad 11$$

Dissociative recombination seems to be the most probable possibility for electron recombination in a proportional counter. Here a radiationless transition occurs to some state of the molecule XY

$$(XY)^+ + e^- \rightarrow (XY)^{**} \rightarrow X^* + Y^* \qquad 12$$

where the asteriks indicate the atom may be left in excited states. The recombination coefficient for this type of recombination amounts between 10^{-6} and 10^{-8} (cm^3/sec), at gas temperatures of 300°K (Ref 26:107). The coefficient for other modes of recombination, or the radiative, dielectric, and three-body recombinations, is on the order of 10^{-10} to 10^{-12} (cm^3/sec) (Ref 26:107). Recombination is significant only in regions where the concentration of ions and/or electrons is dense. At low values of the field and at high gas pressure, recombination will be more severe since the normal diffusion of ions and electrons away from their point of origin is slowed (Ref 8:154).

End Effects, Eccentricity of the Wire

Good energy resolution in a proportional counter is critically dependent on assuring that each electron formed in an original ionization event is multiplied by the same factor in the gas multiplication. This proportionality can be upset by a distortion of the axially uniform electric field. This distortion may be caused by any variation in the diameter of the anode wire along its length, any eccentricity of the wire along the axis of the counter, or even microscopic particles of dust on the anode wire; all of these potential sources of field distortion will vary the degree of gas multiplication. The spread in gas multiplication caused by a given eccentricity of the wire can be determined by

$$\delta E/E = 4a\Delta/b^2 \qquad 13$$

where Δ is the eccentricity of the anode wire,

and from the experimentally determined dependence of the gas multiplication on the electric field strength at the inner electrode (Ref 39:95). Uniformity of the anode wire diameter can be ensured by the use of only high quality anode wire, specifically designed for use in counters. Microscopic particles on the anode wire can be removed by glowing the wire while the counter is evacuated, which also drives off occluded gases and contributes to chemical stability (Ref 40:198).

Distortion from end supports and endplates introduces a serious degree of distortion of the electric field near the ends of the wire. The two chief consequences are 1) the el-

fective volume of the detector is not strictly and accurately related to the length of the central wire, and 2) the variation of electric field near a support results in a fairly extended region (~ the radius of the counter) within which the gas multiplication rises from very low values to the constant value attained in the central volume. Small field-adjusting tubes fitted over the usual grounded guard tubes, and maintained at the potential appropriate to their diameter, reduce end effects to negligible proportions; these tubes need not be longer than the radius of the counter (Ref 41:37). The utilization of field tubes insures a precisely defined volume. When the field tube is adjusted to the potential Vp corresponding to its radius rp, the following relationship holds

$$R = Vp/Vc = \ln(rp/rw)/\ln(rc/rw) \qquad 14$$

where Vp is the field tube voltage, and Vc is the cathode voltage (Ref 41:39).

Other systems for correcting end effects include semiconducting endplates, concentric rings etched on nonconductive endplates and set at suitable potentials, and duplicate counters of varying length (Ref 42, 43, and 44).

Space Charge Effects

Space charge nonlinearities, caused by the gradual diffusion of the positive ions toward the cathode wall, may result in a distortion of the electric field at small radii, and possibly a reduction in the output pulse size and degradation of

energy resolution. There are two different categories of space charge effects. The self-induced space charge effect results from the positive ions in a single pulse discharge retarding the electron cloud at the head of the avalanche; the effect is a function of gas multiplication and tube geometry, not pulse rate. General space charge effects include the cumulative effect of positive ions created from many different avalanches; this effect is important at low values of gas multiplication, and is clearly counting rate dependent. General space charge effects are most prominent in large counters operated at high pressure because the effective counter potential is proportional to $p^2b^3Gln(b/a)$. If a radially uniform space charge is assumed, then the effective counter potential becomes

$$V = Vo - [k\, \eta e p^2 b^3 \ln(b/a) GN]/2\kappa \ell Vo \qquad 15$$

where k = constant

κ = mobility

η = the average number of ion pairs produced per cm of track length per unit pressure

e = electronic charge

ℓ = length of the irradiated length of the counter

N = counting rate

G = gas gain (Ref 32:224).

The use of gas multiplication factors that are as low as possible consistent with signal-to-noise requirements, will avoid potential loss of energy resolution due to [illegible]

effects. Analytical formulations to allow estimation of the resulting nonlinear effects were developed by Hendricks and Champion (Ref 45 and 32).

Resolution

Proportional counter energy resolution depends on many factors including anode wire non-uniformity, electron attachment to gaseous impurities, amplifier noise, and others. Of all of these factors, only statistical fluctuations occurring in the number of primary ion pairs produced by the ionizing particle, and the number of secondary electrons produced in the avalanche initiated by each primary electron, fundamentally limit the resolution and can not be eliminated in principle.

The fluctuations of the pulse amplitude in the proportional counter depend on the variance of primary ionization and gas amplification in the following way

$$(\sigma p/\bar{p})^2 = (\sigma N/\bar{N})^2 + (1/\bar{N})(\sigma A/\bar{A})^2 \qquad 16$$

where $\bar{N}$ is the mean number of the primary ion pairs

$\bar{A}$ is the mean amplification factor

$\bar{P} = \bar{N}\,\bar{A}$

σN, σA, σp are the standard deviations of the previous quantities (Ref 46:31).

The variance of the number of primary ion pairs follows the dependence $(\sigma N/\bar{N})^2 = F/\bar{N}$, where F is a constant characteristic to gases, the so-called Fano-factor (Ref 47). The number of primary ion pairs is determined by another constant specific

for the gas, the mean ionization energy $W = \epsilon/N$, where ϵ is the energy of the quantum to be measured. Using the Polya distribution model proposed by Byrne, the variance of gas amplification for one electron is

$$b = (\sigma A/\bar{A})^2 \qquad 17$$

(Ref 8:199).

Combining the above equations one obtains the well-known fact that in the absence of electronic noise, relative deviation of pulses is dependent on the square root of the energy to be measured

$$\sigma P/\bar{P} = [(F+b)W/\epsilon]^{1/2} \qquad 18$$

(Ref 48:251).

The pulse amplitude variance is dominated by fluctuations in avalanche size, and fluctuations in the original number of ion pairs is a small contributing factor (Ref 48:251). The peak width expressed in percentage of maximum is the so-called resolution, and in the case of a Gaussian distribution it is 236 $\sigma P/\bar{P}$%. To optimize resolution, the quantity (F+b)W must be minimized. A rather profound analysis of both Fano-factors and the variance of gas amplification has been done by Alkhazov et al. (Ref 49 and 50). Table VIII lists resolution-related constants for some proportional gases. Note that certain gas mixtures, e.g. Ne + 0.5% Ar and Ar + 0.5% C_2H_2 are especially interesting. The excited atoms of the main gas that are born in the absorption of the [illegible]

ionize the atoms of the minor gas, hence a strongly decreased mean ionization energy and Fano-factor result.

Table VIII. Resolution-Related Constants for Proportional Gases at Atmospheric Pressure (Ref 8:201).

Gas	W (eV/ion pair)	Fano Factor calc	exp	Multiplication Variance b
Ne	36.2	.17		.45
Ar	26.2	.17		.50
Xe	21.5		$\leq$.17	
Ne+.5%Ar	25.3	.05		
Ar+.5%C_2H_2	20.3	.075	$\leq$.09	
Ar+10%CH_4	26	.17	$\leq$.19	.50

To achieve the ultimate in proportional counter resolution, one must use 1) the smallest possible voltage and gas amplification, 2) a gas pressure and radius of anode wire such that the product p*a is as low as possible, and 3) certain gas compositions which increase ionization and decrease the variance of the gas amplification (Ref 51:89). For a high pressure counter, these are somewhat conflicting requirements.

Spurious Pulses and Afterpulses

The optical radiation emitted from excited atoms in the Townsend avalanche causes the ejection of a photoelectron from the cathode. This photoelectron will then drift toward the anode, creating another avalanche and producing a spurious pulse, which will be delayed from the primary pulse by the electron transit time required to drift from the cathode to

anode. The incidence of spurious pulses decreases as the anode diameter increases, and also depends on the counting gas (Ref 52:75). Knowledge of the onset of spurious pulses can be used to detect the "end" of a plateau.

Time delayed pulses initiated by a primary ionizing event (afterpulses) are extremely small in the proportional counter, and fall into the region mainly below 100 eV; their origin is not completely understood. Possible causes include negative ion formation, positive ion formation, metastable atomic states of the counter gas, and field emission (Malter effect) (Ref 53:195).

Time Characteristics of the Signal Pulse

Virtually all the charge generated within the proportional tube originates within the avalanche region, regardless of where the original ion pairs are formed. The time history of the output pulse is divided into two stages 1) the drift time required for the free electrons created by the radiation to travel from their original position to near the anode wire where multiplication can take place, and 2) the multiplication time required from the onset of the avalanche to its completion (Ref 8:203). The effect of the drift time is to introduce a delay between the time of formation of the ion pair, and the start of the corresponding output pulse. The drift time (~1 microsecond) is much greater than the multiplication time, and varies depending on the radial position of the original ion pair within the tube. The bulk of the

output pulse is attributable to the drift of the positive ions, since most of the ions and electrons are created close to the anode wire. The positive ions initially move rapidly in a high field region, leading to a fast-rising initial component of the pulse. At greater radii their drift velocity decreases with the field, thus the latter part of the pulse rises very slowly and may not be seen due to the finite shaping of electronic circuits (Ref 8:203).

For a cylindrical cathode enclosing a wire anode, the anode pulse is described by

$$\Delta V_a(t) = B \ln(1 + t/t_o) \qquad 19$$

where $B = -N_o A e/[2C\ln(b/a)]$ 20

$t_o = [a^2 \ln(b/a)]/[2V_o \kappa_o (p_o/p)]$ = a characteristic time 21

t = time from the start of the multiplication

with V_o = static anode voltage with no ionization present in the counter

ΔV_a = change in anode voltage from Vo

N_o = number of ion pairs produced by the primary ionizing event

A = gas gain of the counter (number of avalanche electrons divided by number of primary electrons)

e = charge of electron

C = capacitance of counter

b = cathode radius

a = anode radius

p = pressure of filling gas

κ_o = ionic mobility (the proportionality constant in the equation relating the positive ion drift velocity μ_D to the electric field E at a standard pressure p

$$\mu_D = \kappa_o E$$

(Ref 54:227).

Since all original ion pairs are not formed at a fixed radius, the spread in electron drift times will introduce additional spread in the rise time of the output pulse. Figure 10 shows the shape of the expected leading edge of the output pulse under two conditions 1) ion pairs formed at a constant radius, and 2) ion pairs uniformly distributed throughout the volume

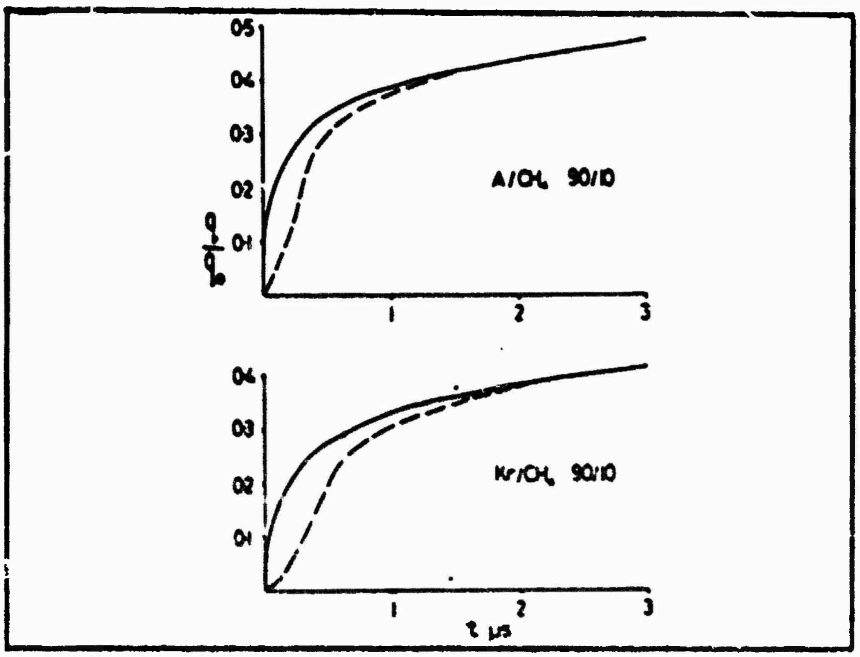

Figure 10. Proportional Counter Profiles for 1) Localized Ionization (solid lines), and 2) Uniform Initial Ionization Along a Counter Diameter (dashed lines) (Ref 55:159).

of the counter. When pulses from proportional counters are shaped using time constants of several microseconds, the slow drift of the ions no longer contributes to the pulse amplitude. The shaped pulse therefore has an amplitude which is less than that corresponding to an infinite time constant by an amount known as the "ballistic deficit."

IV. Design and Construction of Detectors and Gas Handling System

Introduction

An ideal proportional counter acts as an energy transducer and linear amplifier - the charge collected on the anode wire is proportional to the energy of the incident photon. This ideal is never quite met in practice, but with careful design and suitable operating conditions it can be approached. The primary objective in the design of a proportional counter is good energy resolution. Energy resolution is greatly affected by the uniformity of the electric field around the anode wire in the sensitive volume. Design criteria favoring uniformity of the electrical field are a symmetrical wire, and cylinder design having an axial location of the anode wire mounted for minimum end effect. As discussed in Chapter III, the advantage of cylindrical geometry lies in the fact that the Townsend avalanche takes place in a much shorter time interval. This chapter converts the myriad of proportional counter theory presented earlier into design and construction specifications for two high pressure proportional counters, and associated gas handling equipment.

Design of the First Detector

The first detector was modeled after a high pressure proportional counter constructed by R. Batchelor et al. to

measure fast neutron spectra in a helium-3 medium (Ref 12:1037). The selection of operating pressure was determined by the radiation energy, and the discrimination range desired. Figure 11, prepared from calculations of linear energy transfer for electrons in gases, shows that an electron of energy greater than 200 keV may at atmospheric pressure, deposit less than 10 keV/cm in the detector using xenon as the medium. If discrimination over a range of zero to about 200 keV is

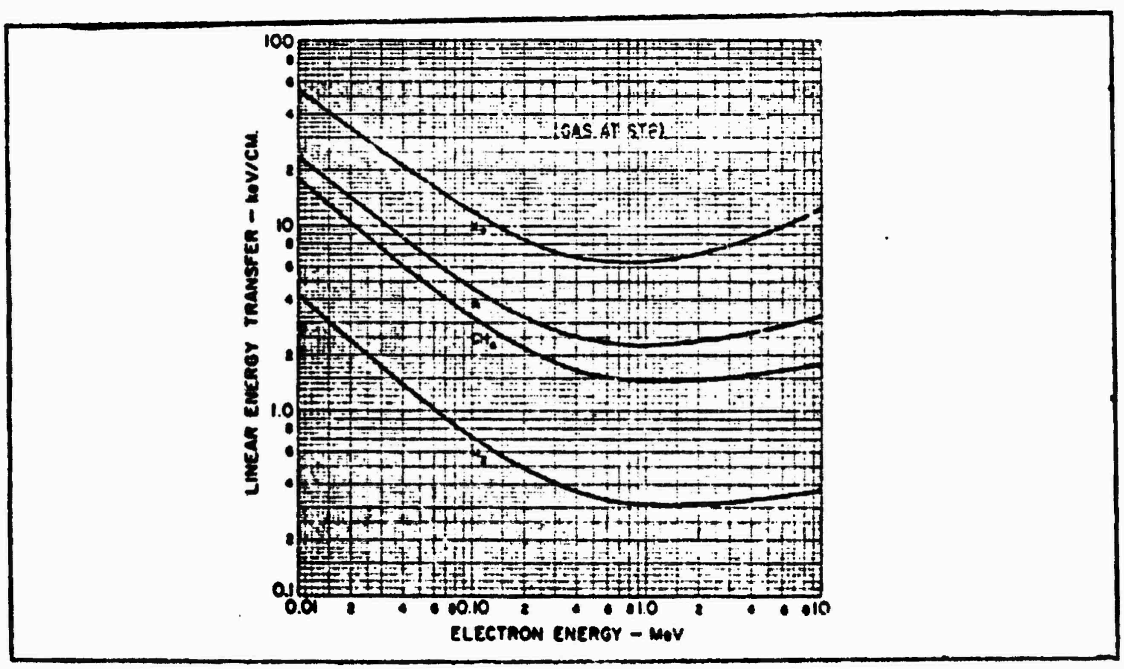

Figure 11. Linear Energy Transfer for Electrons in Gases (Ref 10:96)

desirable, an operating pressure of 20 atm would be adequate for most beta emitters. The linear range of electrons is also very useful for a more specific choice of pressure as presented in Figure 12 below.

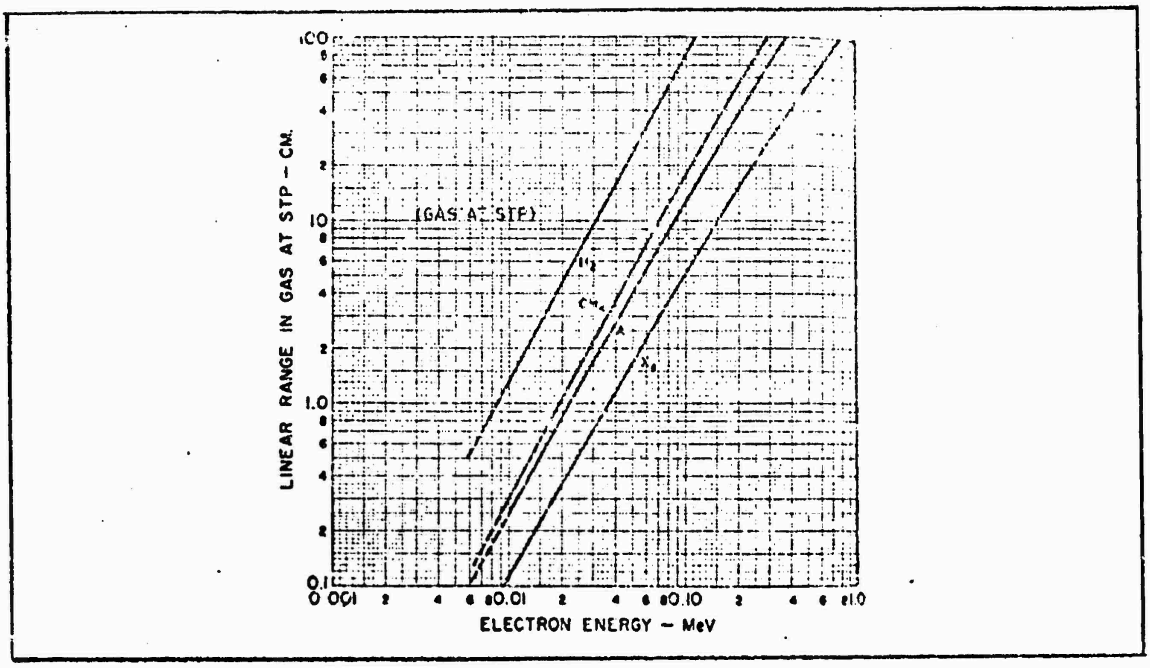

Figure 12. Linear Range for Electrons in Gases (Ref 10:96)

Expanding on Figure 12, the range of 160 keV electrons in xenon is 56.8 mg/cm^2; the density of xenon is 5.887 g/l (Ref 22:14). The range in cm required to stop 160 keV electrons in xenon as a function of pressure is shown in Table IX.

Table IX. Range in cm Required to Stop 160 keV Electrons in Xenon as a Function of Pressure

Pressure (atm)	1	5	10	20	30	40	50
Range (cm)	10.75	2.15	1.08	0.54	0.36	0.27	0.21

The high particle stopping power of xenon is amply demonstrated in a comparison of the range in cm required to stop, for example, 230 keV electrons in other counting gases in Table X below.

Table X. Range in cm Required to Stop 230 keV Electrons in Counting Gases as a Function of Pressure (Ref 22:34)

Pressure (atm)	1	10	20	30
Argon				
Density(g/l)	1.784			
Range (cm)	33.6	3.36	1.68	1.12
Methane				
Density(g/l)	0.554			
Range (cm)	108.0	10.8	5.4	3.6
P-10 Gas				
Range (cm)	41.0	4.10	2.05	1.37
Xenon				
Density(g/l)	5.88			
Range (cm)	18.8	1.88	0.94	0.63

In Figure 13 argon pressures required for various degrees of photon absorption are shown. The useful response of xenon can be extended appreciably above the photon energies shown for argon (Ref 8:209).

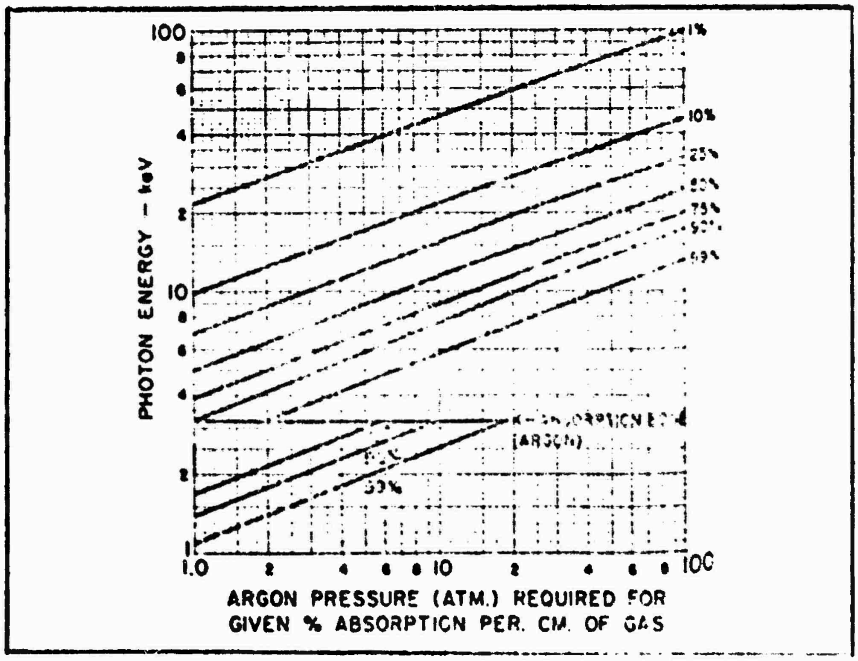

Figure 13. Photon Attenuation in Argon Gas

Using the information detailed above, a pressure of 50 atm and cathode radius of 2.05 cm were utilized in the design and operation of both detectors, ensuring that the conversion electrons of ^{131m}Xe and ^{133}Xe and the average energy of the beta spectrum of ^{133}Xe is deposited in the sensitive volume of the detector.

A diagram of the first detector is shown in Figure 14. The body of wall thickness .20 in., was machined from stainless steel 303 and threaded at each end. Endplates which carried insulator and electrode assemblies were screwed into the ends, and sealed using a teflon washer and brass holding ring. The endplate design was similar to that described by Cockroft and Curran, but in this case the joints were designed to withstand pressures of more than 75 atm. in the counter (Ref 41). Design computations for the thickness of stainless steel 303 and 304 construction parts under the maximum internal pressure were made using the formula

$$t_m = (PD/2S + YP) + C \qquad 22$$

where t_m = minimum pipe wall thickness (in.)

P = maximum internal service pressure, p.s.i.g.

D = O.D. of tube (in.)

S = allowable stress in material

Y = variable coefficient (Ref 56:8-207)

C = allowance for threading, mechanical strength, and corrosion (in.)

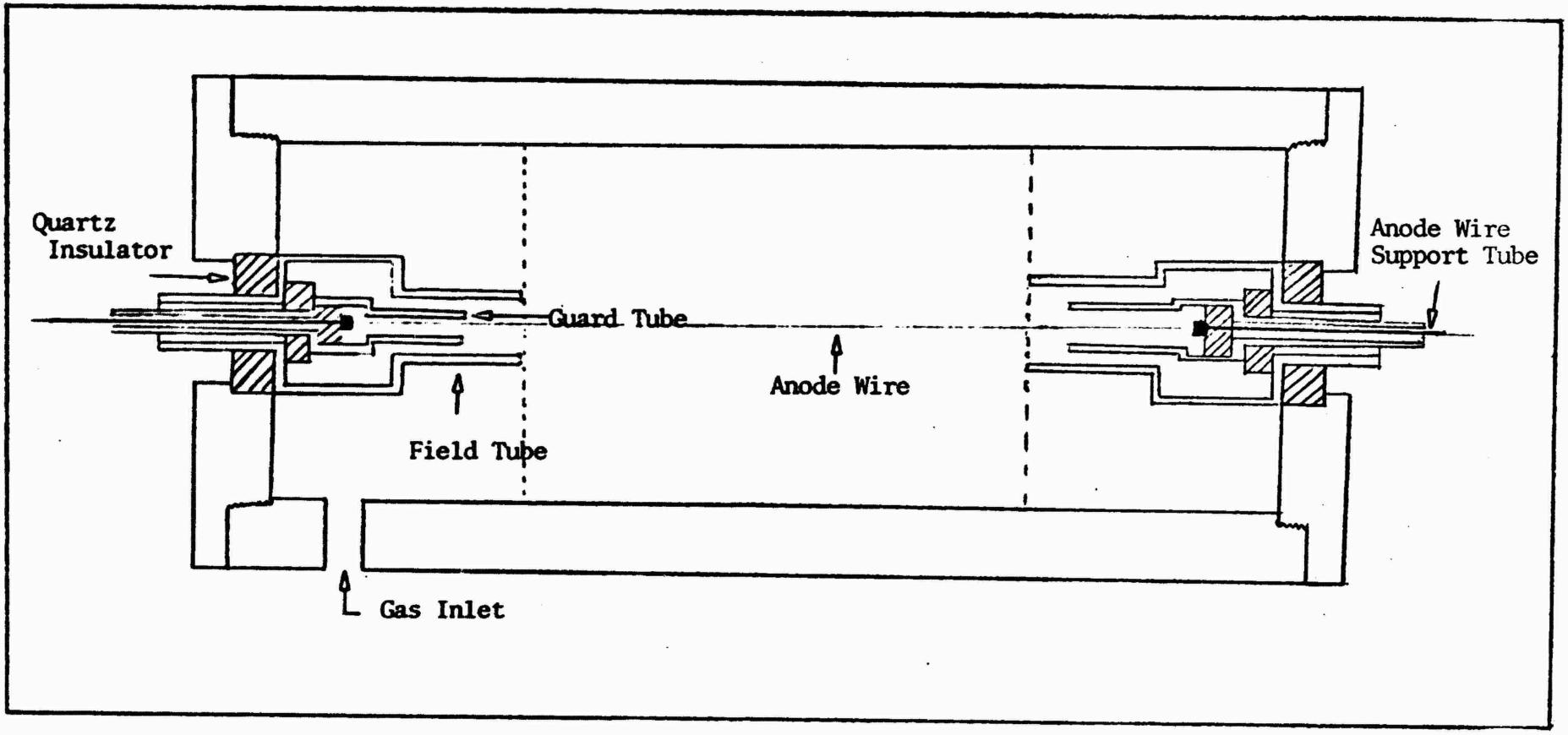

Figure 14. First High Pressure Proportional Counter

Quartz rings were used as insulators in the first detector, and were bonded to the stainless steel endplates, field tubes, guard tubes, and anode wire support tubes with Varian torr-seal. Each quartz ring was located in a recess to make all the electrodes concentric. The guard tubes and field tubes were composed of two separate sections for ease of construction, which threaded together. The anode wire was stainless steel 302, 0.0004 in. and 0.0005 in. diameter. The ends of the counter were electrically screened with brass covers connected to the cathode but isolated from instrument ground. The relevant dimensions of the counter were diameter (I.D.) 1.61 in., total length 5.25 in., field tube diameter 0.25 in., field tube length 0.563 in., guard tube diameter 0.125 in., and sensitive volume 80 cc. A complete description of the first detector is presented in Appendix A.

The use of a very thin anode wire presents potential liabilities such as loss in resolving power from specks of dust that may accumulate on the wire, and from possible nonconformity of wire diameter along the length of the sensitive volume of the counter chamber. Very thin anode wires are also very difficult to mount without breaking. However, since the gains from the use of thin wires are very real, and the potential liabilities could be minimized, the choice of 0.4 and 0.5 mil diameter wire was made. Since the field strength at the anode wire (and consequently multiplication factor) is a function of wire diameter and potential difference between the wire and cylinder wall, the use of a very thin anode wire per-

mits a lower operating voltage with attendant gains in stability through the reduction of electrical leakage. From the Diethorn semi-empirical formula for gas multiplication

$$\ln M = \frac{V}{\ln(b/a)} \cdot \frac{\ln 2}{\Delta V} \left[\ln \frac{V}{pa\ln(b/a)} - \ln k\right] \qquad 23$$

and the design specifications for the first detector, the importance of an extremely thin anode wire for high pressure proportional counters can be shown (Ref 45:309). Using the Diethorn parameters for Xe - 10% CH_4, and a gas multiplication of 100, the applied potential (volts) using a 0.4 mil anode wire is approximately 9400 volts; for a 0.5 mil and 0.2 mil wire the applied potential is 11000 volts and 6000 volts respectively! The variation with multiplication with applied potential and anode wire diameter for a mixture of xenon and two different quench gases is presented in Table XI. Note that for the parameters specified for the counter, the smaller the anode wire diameter, the lower the applied potential for a multiplication of 10^2-10^4. Limitations imposed by electrical breakdown usually restrict useable voltages to less than 10 kV, and anode diameters to less than about 100 μm (Ref 10:96).

Table XI. Variation of Multiplication with Potential and Anode Wire Diameter

Gas Mixture	Applied Potential (v)	Multiplication Anode Wire Diameter (in.) 0.0002	0.0004	0.0005
90%Xe/10%CH_4	9000	8.2×10^6	387	0.49
	10000	5.3×10^8	780	6.57
	11000	4.2×10^{10}	2.0×10^4	1.13×10^2
95%Xe/5%CO_2	9000	2.3×10^7	398	0.36
	10000	2.0×10^9	990	5.65
	11000	2.2×10^{11}	3.2×10^4	1.18×10^2

Design Problems with the First Detector

The major design problem with the first detector was the impossibility of obtaining the proper material for construction. Batchelor's original detector design utilized 36% nickel-iron (invar) for the endplates, anode wire supports, and the initial half of the guard and field tubes. The body of the counter was constructed of stainless steel. The guard tubes and field tubes which were screwed onto the nickel-iron tubes, were made of Dural (Ref 12:1039). Invar was specifically used in all metallic parts requiring bonding to the quartz insulators with Araldite. The coefficient of thermal expansion of invar is 0.8×10^{-6} cm/cm^{o}C, which is very close to that of quartz, 0.55×10^{-6} cm/cm^{o}C. Stainless steel, however, has a coefficient of thermal expansion of 21.78×10^{-6} cm/cm^{o}C (Ref 58)! Batchelor was therefore able to screw and soft solder the endplates into the body without weakening the Araldite seams (Ref 12:1039). Since invar could not be obtained,

stainless steel 303 was utilized for all metallic parts of the first detector. The high pressure constantly initiated small leaks around the endplates, and at various stainless steel and torr-seal joints. Repeated attempts to repair leakage soon altered the detector into a highly impractical proportional counter. It was extremely difficult to remove the endplates to replace anode wires, due to the great amount of torque which had been required for a proper seal to the counter body, and to additional torr-seal utilized as leak sealant.

Other design flaws included the threaded endplates, the instep for the large quartz insulator, and the eccentricity in the concentric alignment of guard and field tubes, and anode wire support. The threads on the endplates and counter body were sources of virtual leaks. The only solution was to coat the threads with high vacuum epoxy, but this would introduce organic impurities and would have compounded the problem above. The seat for the large quartz insulator did not provide enough spacing between the cathode and field tubes. Original design specifications delineated much greater spacing, which was reduced to aid in alignment of the field tubes. The concentric field tubes, guard tubes, and anode wire supports were also very difficult to align properly while epoxying the stainless steel parts and quartz insulators. This was caused by the non-parallel ends of the quartz rings, and the omission of plexiglass inserts to properly center all tubing during bonding. The detector was also very sensitive to radio frequency (RF) interference. Apparently the brass

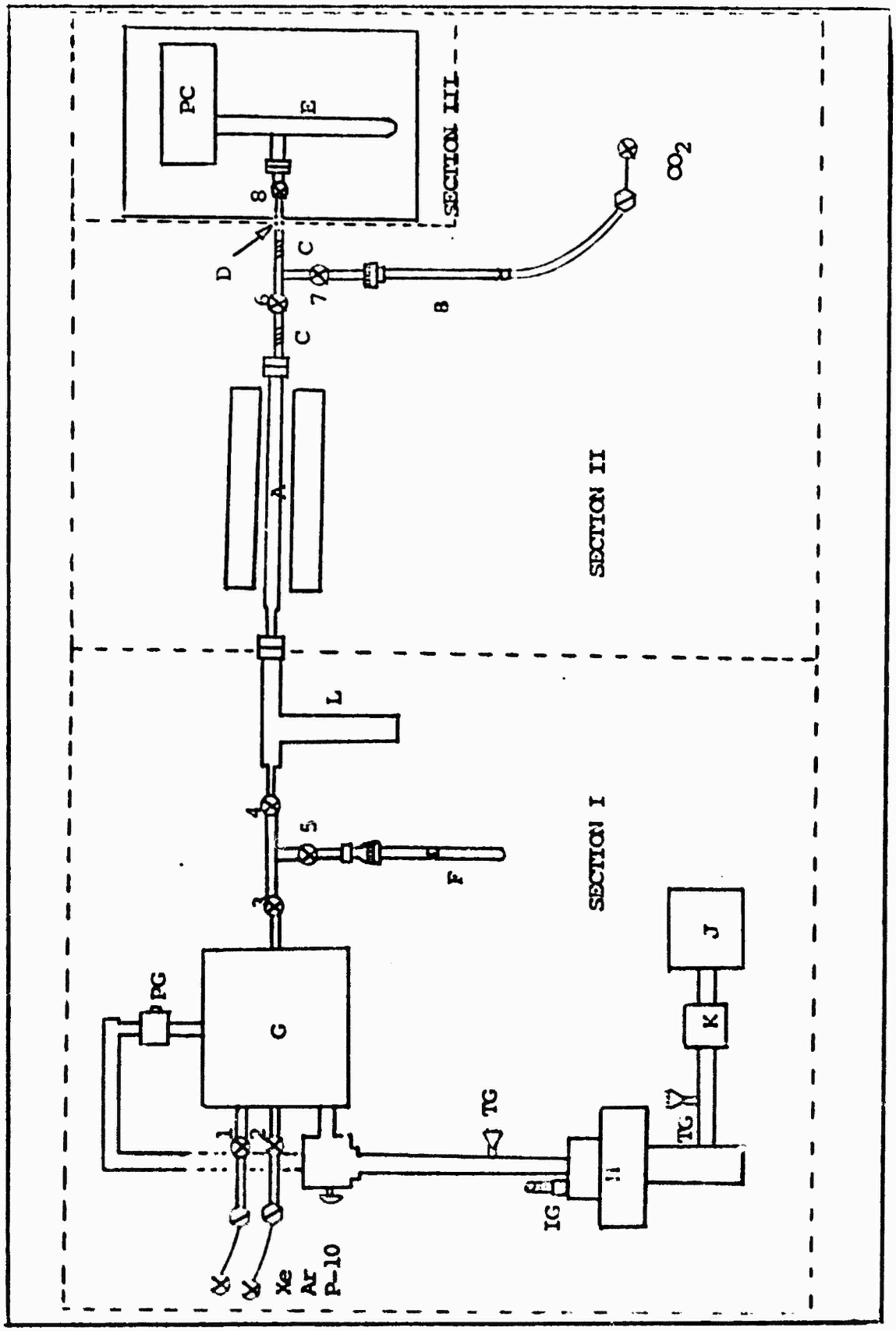

Figure 15. Gas Handling System and General Configuration

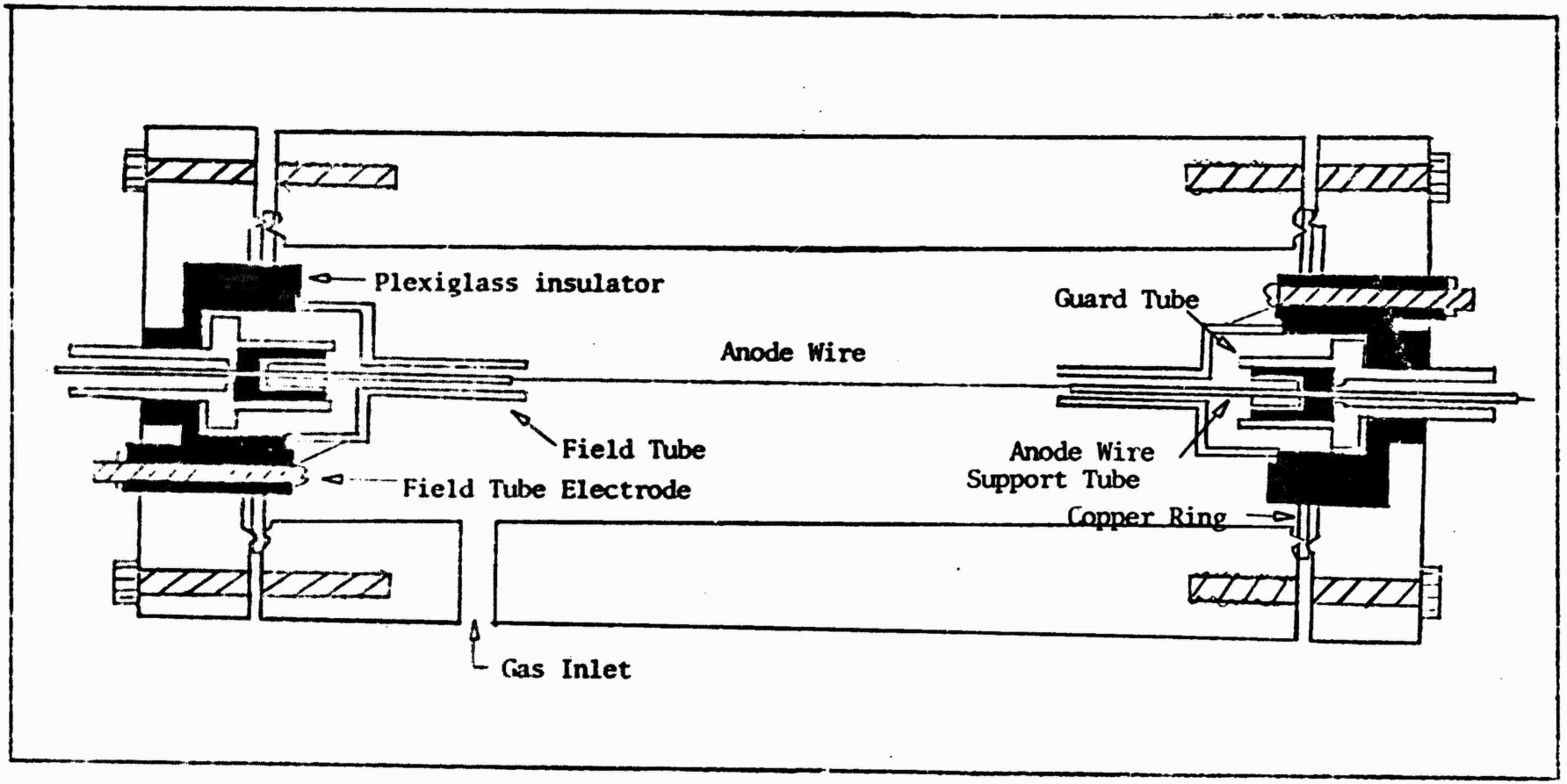

Figure 16. Second High Pressure Proportional Counter

end caps were not very effective in electrically screening the counter.

The first detector never was operated successfully at atmospheric or high pressure. The counter displayed excessive noise whether operated with the anode at positive potential, or with the cathode at negative potential. Many of the problems could only be eliminated by redesign.

Design and Construction of the Second Detector

Figure 16 is a drawing of the second detector. Figures 17, 18, and 19 are photographs of the first detector, second detector, and gas handling systems respectively. Appendix A contains a detailed description of the components and materials used.

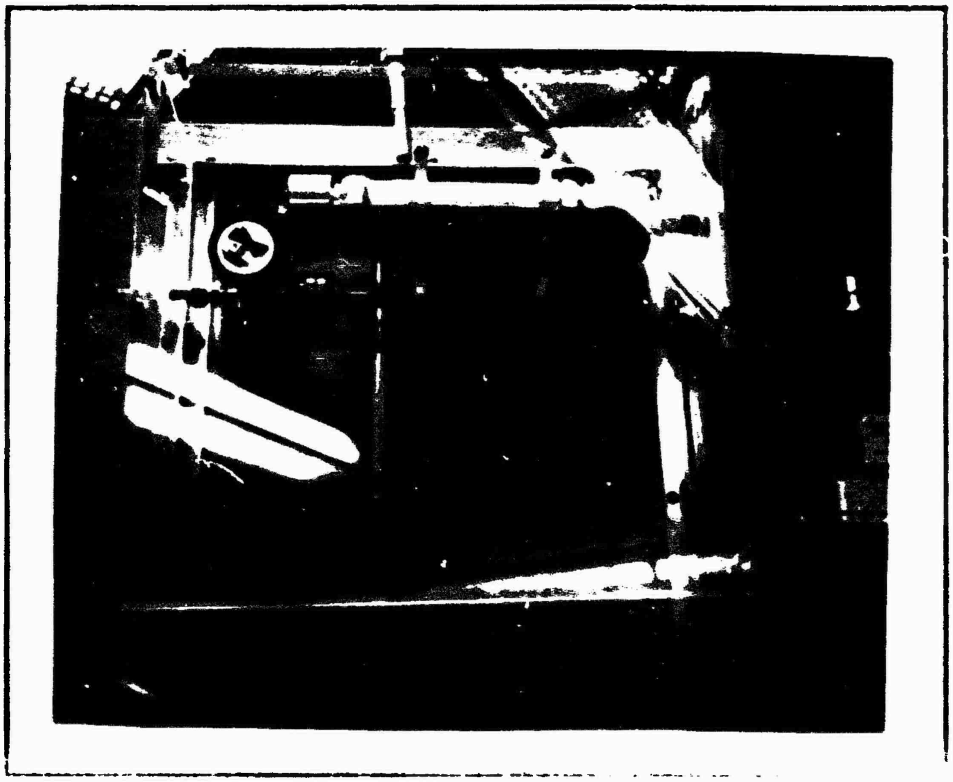

Figure 17. First Detector

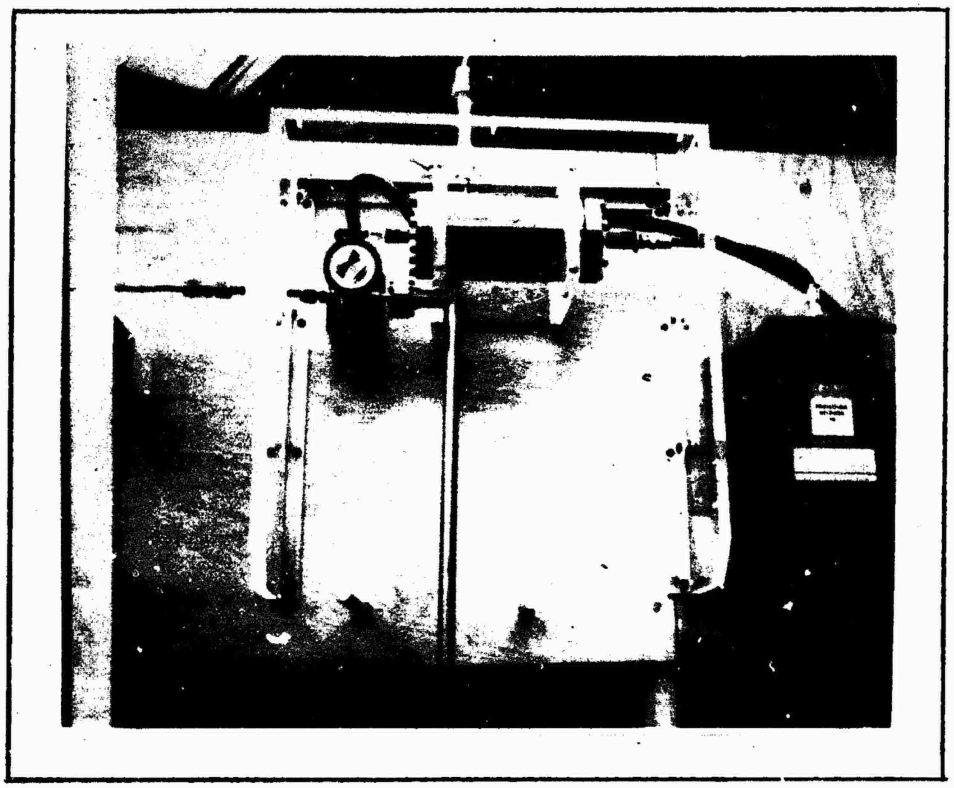

Figure 18. Second Detector

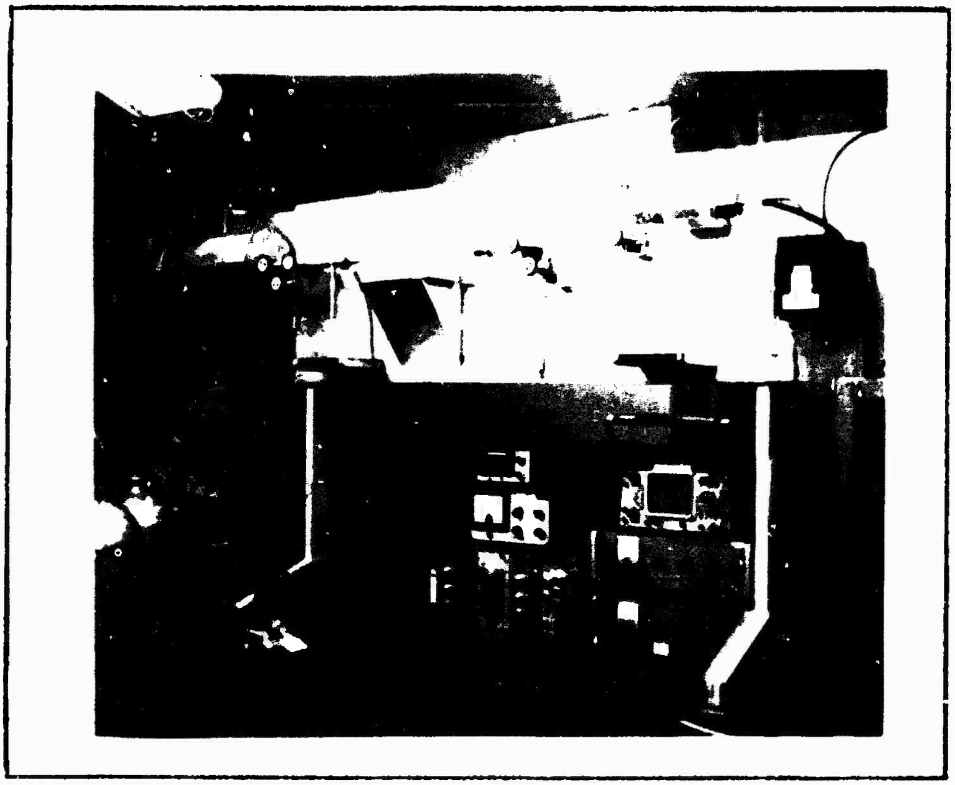

Figure 19. First Detector and Gas Handling System

The second detector utilizes a flange-type connection for the endplates and counter body, and is vacuum and pressure sealed on both ends by a knife-edge and soft copper ring. The body of wall thickness 0.688 in., is machined from stainless steel 304. The cold finger is heliarc-welded both in the interior and exterior of the counter; the first cold finger was threaded into the first detector, and later silver soldered. Three plexiglass insulators were machined for each endplate for a perfect torr-seal joint with the stainless steel parts. The relevant dimensions of the counter are: inside diameter 1.625 in., total length 5.25 in., field tube length 0.8125 in., guard tube diameter 0.50 in., field tube diameter 0.30 in., wire support tube diameter 0.058 in., anode wire diameter 0.0005 in., and sensitive volume 70 cc. The concentric electrode connections are avoided in detector #2 by using a brass screw which threads through the endplate and makes an electrical connection to the field tube inside. Field tube length is exactly the radius of the counter (Ref 41). Alignment of the field and guard tubes, and the anode wire support tube is extremely simple due to the exact construction of end pieces, and the use of plexiglass inserts while bonding.

Design Problems with the Second Detector

The only design flaw found in the detector was inadequate insulation for the guard tube outside of the counter. When the detector is used at high pressure at a cathode potential of [illegible] an electrical discharge appears between

one endplate and the exterior guard electrode; this occurs only on the side of the detector where the anode wire and guard tube are connected via a short cable to the preamplifier. Another potential problem is the sharp edges on the six screws holding the endplate against the counter on the same side. Teflon insulators were made for all six screws, and for the external guard tube. In addition, corona dope was painted on the exterior surface of the endplate. This insulation did not terminate the discharging, only making it extremely sporadic. The electrical discharge from the endplate to the guard tube limited the negative potential of the cathode.

Gas Handling System and General Configuration

Figure 15 shows the schematic arrangement of the filling and pumping section (I), the purification section (II), and the detection section (III). Swagelok fittings and Varian knife-edge flanges are utilized whenever possible in all sections, thereby eliminating the necessity of soldering.

Section I includes: a gas reservoir of known volume (G), a pressure gauge (PG), Nupro valve inlets for counting gases (valves #1,#2), a reservoir for cryogenic pumping (L), a Nupro valve inlet and breakseal tube for radiation samples (F, valve #5), gas flow control valves (valves #3,#4), and a high vacuum system consisting of a forepump and diffusion pump (J and H), a zeolite filter (K), four vacuum valves (only one shown), an ionization gauge (IG), and two thermocouple [illegible] (TC).

tion III consists of the proportional counter (PC), a reservoir for cryogenic pumping (E) and a specially designed, high pressure Nupro valve (valve #8). A 1/2 inch thick lucite shield covers section III, providing blast and high voltage protection for lab personnel.

The cold fingers (E and L) in sections I and III are used to cryogenically transfer the proportional counting gases, and the radioactive xenon sample into and out of the detector and purification train. Ultrapure argon, P-10 (90% argon, 10% methane), and ultrapure xenon gases were used during this study. The critical volumes of the gas reservoir, the cold fingers, and the detector were calculated using both the ideal gas law and the Van der Waals equation. These components were designed and constructed so that one atmosphere of xenon gas in the reservoir (G) volume would expand to 50 atm. at room temperature in the smaller combined volumes of the detector (PC) and cold finger (E) after being cryogenically transferred from the reservoir (G) and condensed into cold finger (E) at liquid nitrogen temperature. The gas reservoir was designed and constructed with a 12.4 liter volume; the combined volume of the detector and cold finger was 201 cm^3. Approximately 40% of a radioactive sample, excluding cryogenic transfer losses, will be in the sensitive volume of the detector. A 0-25 p.s.i.d. pressure transducer is attached to the gas reservoir to determine the pressure of the proportional gas in the reservoir before transferal to the detection. The volumes of all system components were calibrated

using a reference flask of known volume, 1058.29 $\pm$ .24 cm^3. While both forepump and diffusion pump are operating, the system can be evacuated to $4x10^{-7}$ torr.

Section II is composed of: a purifier (A) heated by a double element, tubular furnace, a drierite (calcium sulfate) container (B), an inlet for CO_2 or any quench gas (valve #7), two stainless steel bellows (C), a glass insulator (D), and a gas flow control valve (valve #6). The purifier is a quartz tube filled with zirconium-titanium turnings. The purifier is operated at 1000°C; at this temperature oxygen is removed completely, and nitrogen is reduced to 0.10% (Ref 57:296). The stainless steel bellows are used to prevent excessive torque on the purifier and the high voltage glass insulator during assembly and disassembly. Drierite is used for drying high-purity CO_2 or any quench gas. Research purity CO_2 gas was not obtained in time for use during this study.

Electronics

The electronics used with both detectors are shown in Figure 20. Two Power Designs regulated high voltage power supplies are used to provide a negative bias of 1-30 kV for the cathode, and 1-10 kV for the field tubes. The pulses from the proportional counter are processed by an Ortec preamplifier, and then shaped and amplified by an Ortec linear amplifier. The preamplifier is mounted near the detector. Cable connections between the anode wire and guard tubes, and the preamplifier are additionally shielded by teflon and

phenolic insulators.

The monopolar signals from the linear amplifier are fed into a single channel analyzer and to a multichannel analyzer. The multichannel analyzer is linked to a plotter, and a teletype. An oscilliscope is used to monitor the output of the preamplifier and the amplifier. The output of the single channel analyzer is connected to a scaler/timer.

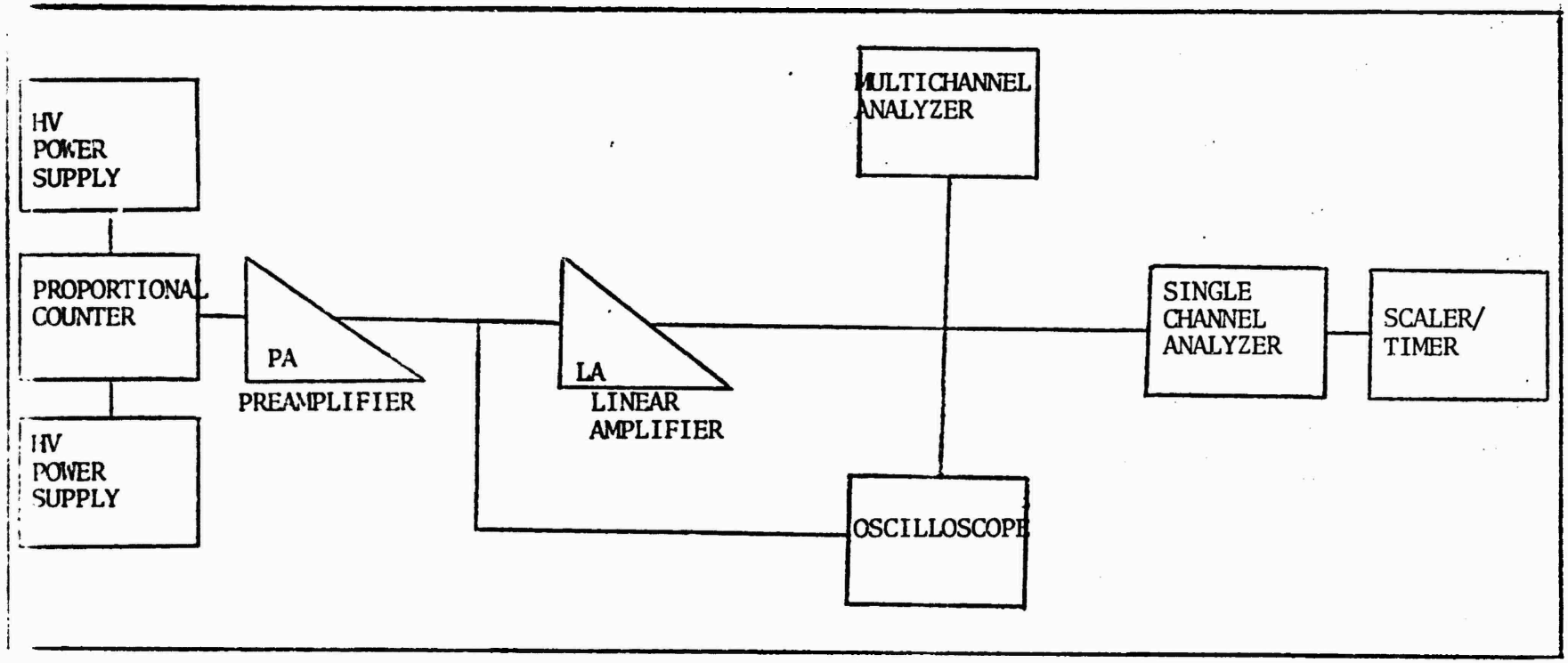

Figure 20. Detection System Electronics

V. Operation, Operating Characteristics, and Results

Introduction

The experimental results of this research are presented in this section. First the preparation for system operation is discussed. Next the operation of the detection system with both detectors and the gas handling system is discussed. The operating characteristics of both detectors are presented. Finally sample energy spectra characteristic of three radionuclides are shown for operation at both atmospheric and high pressure.

Assembly of the System

Before assembling the gas handling system, components were thoroughly degreased, and soaked or ultrasonically cleaned. The forepump and diffusion pump were used to continually evacuate the detection system. The purifier was outgassed at 1000°C for a minimum of 8 hours before flushing the system with argon prior to filling it with xenon or argon. The cylindrical interior cathode surface of the detector is polished to a mirror finish, and component parts are also degreased and ultrasonically cleaned.

The counter is assembled in a dust free environment. The very fine anode wire is installed with infinite care using the following systematic procedures. After threading a 0.02 in. outside diameter (O.D.) stainless steel tube through the

detector, a small drop of cyanoacrylate is used to attach the anode wire to one end of the tube. After the cyanoacrylate sets, the tube is pulled through the detector, thus threading the anode wire. Next the 0.041 in. interior diameter (I.D.) anode wire support tube at one end of the counter is plugged with a brass insert 0.2 inch long. A 0.059 in. O.D. brass cap with a tip is fit over the anode wire support tube and brass insert, and bonded with torr-seal. Since axial asymmetry of the anode wire causes a loss in resolution, the wire was tensioned with approximately 5 grams at the other other end and capped similarly. The breaking tension of the 0.5 mil wire was found to be approximately 14 grams. The excess wire protruding beyond the epoxy seal was then clipped. After installing the counter in the detection system, the center wire was flashed twice in a vacuum at a current of 50 milliamperes for two seconds each time.

System Operation

The operation of the two detectors is essentially the same. After the system is evacuated, the ultrapure argon is used to flush the system. One atmosphere of the xenon counting gas is transferred into the gas reservoir. The radioactive xenon sample is initially frozen by immersing the breakseal tube in liquid nitrogen, and then after breaking the seal is cryogenically transferred into the first cold finger (L). The xenon sample and counting gas are next cryogenically pumped through the purifier into the detector cold finger (J).

When the xenon vapor pressure is at approximately 1.39×10^{-4} torr, the high pressure valve for the detector and cold finger is tightly closed, and the cold finger allowed to warm to room temperature. Table XII lists the vapor pressure of solid xenon between its freezing point of 161 K to the boiling point of liquid nitrogen. As the temperature

Table XII. Xenon Vapor Pressure (Ref 19:800)

Temperature ^{o}K	Pressure (torr)
70	1.39×10^{-4}
80	4.24×10^{-3}
90	5.99×10^{-2}
100	4.95×10^{-1}
110	2.76
120	11.5
130	38.2
140	101
150	258
160	562

in the cold finger rises to room temperature, the vapor pressure of xenon also rises. If the volume and pressure of xenon are selected correctly, the pressure in the detector will be 50 atmospheres at room temperature ($300^{o}K$). Since proportional counters are well known to deteriorate with prolonged use and ultimately become quite useless, the system may later be reversed, and the xenon periodically passed through the

purifier to rid the gas of electronegative impurities. The anode wire of the proportional counter is connected via a short RG-58c cable to the preamplifier input, which is maintained at ground potential. The cathode and field tubes are held at a high negative potential by well regulated high voltage supplies. Application of this high voltage to the counter can result in EHT breakdown if certain precautions are not taken. All insulators carrying high voltage, particularly those on the counter, must be clean and dry, and the counter must be used in a dry environment (Ref 52:80).

Operating Characteristics of the First Detector

Much time was repeatedly spent correcting the high pressure leaks and design flaws in the first detector as described in Chapter IV. Early operation of the detector at atmospheric pressure using both P-10 and argon fill gases was characterized by extremely weak or no response to external gamma sources. The basic design concepts for the first detector are sound when the proper construction materials are utilized; Batchelor operated a similar detector very successfully at a pressure of 40 atm. for neutron spectroscopy (Ref 12). The first detector, however, could not be operated successfully and experienced the following problems: weak epoxy bonding, virtual leaks, improper sealing of the endplates, insufficient component spacing, poor electrode alignment, radio frequency (RF) interference, and difficult anode wire replacement. All [illegible] the difficul[illegible]

detector were unsuccessfull. Complete disassembly and refabrication of components would have been necessary to correct the problem.

Operating Characteristics of the Second Detector

Most of the inadequacies of the first detector are corrected in the second. The second detector operates both at atmospheric and high pressure without leaking so that the counting gas may be stored in the detector for days without a measureable loss.

The response characteristics of the second detector deteriorated with time because outgassing introduced impurities. Periodic or perhaps continuous purification is definitely required to maintain good resolution and constant multiplication, especially when operating at high pressure. In the early stages of deterioration the spectrum may break into several small peaks, accompanied by a large loss of overall gain. The phenomenon is not well understood, but if organic impurities are present may be associated with deposits on the anode wire (Ref 10:94). Traces of diffusion pump oil, and vapors from the epoxy may also have introduced impurities.

Normal high voltage practice includes component spacing, smooth joints, and insulator cleanliness. While careful attention was given to these requirements in designing and constructing the detector, an external electrical discharge problem developed between the endplate and guard tube electrode as discussed in Chapter IV. The use of corona [illegible],

and teflon and phenolic insulators reduced the frequency of occurrence of the discharge. The early onset of the high voltage discharge outside the detector made it impossible to reach the voltage necessary for an increased gain. Electrical discharging was also initially discovered in the glass insulator and quartz purifier because of the presence of a small amount of xenon in the gas handling system, which had not been cryogenically pumped into the detector cold finger. A CVC thermocouple gauge should be added in section II of the detection system to prevent the recurrence of this problem. The discharge was stopped by evacuating the gas handling system during detector operation.

Results Using the Second Detector

A 0.32 microcurie ^{133}Xe source was transferred into the detection system from the breakseal valve; the activity was 75 disintegrations per second. While cryogenically pumping the sample into the system and subsequent mixing with the xenon medium, the breakseal tube was blown from its o-ring seal due to excessive pressure in the system with the gas reservoir closed. An undetermined quantity of sample and approximately 1/3 of the xenon was lost to the atmosphere, although the Nupro valve to the breakseal tube was immediately closed. Some impurities may also have entered the system at this time. Insufficient ultra-pure xenon remained in the supply bottle to compensate for the xenon lost; consequently, the final pressure in the detector was approximately 41.5 atmospheres.

Since the research purity CO_2 was not available, a quench was not used but must be considered during future studies. As described in Chapter III, a pure noble gas may not be stable at high pressures, especially if multiplication exceeds 100.

The electron spectra for ^{133}Xe is presented in Figure 21. Note the presence of the K shell internal conversion electron and K x-ray summing peak; the resolution (FWHM) of the sum peak is 7.0 keV. The resolution of the 45 keV conversion electron peak is 5.9 keV. The effects of time and purity can be seen in Figure 22. Both spectra were taken with no change in the bias voltage applied to the cathode and field tube; however spectrum B was taken 150 minutes after A. Horizontal and vertical scales and counting times are identical for the spectra. The most significant effect is the decrease in resolution with increasing impurity. The impurities appear to spread the peak pulses over the lower channels, with some of the pulses lost below the lower level discriminator of the multichannel analyzer.

None of the ^{133}Xe spectra contained the predicted number of counts, more of the sample had been lost to the atmosphere than expected. The detector resolution definitely showed that electronegative impurities in the gas filling, perhaps a small amount from the blown breakseal tube, and most liberated from the counter walls negatively influenced the counter performance. The suppression of these impurities will definitely improve the counter characteristics, [illegible] length and rise of the plateau, detection efficiency, and

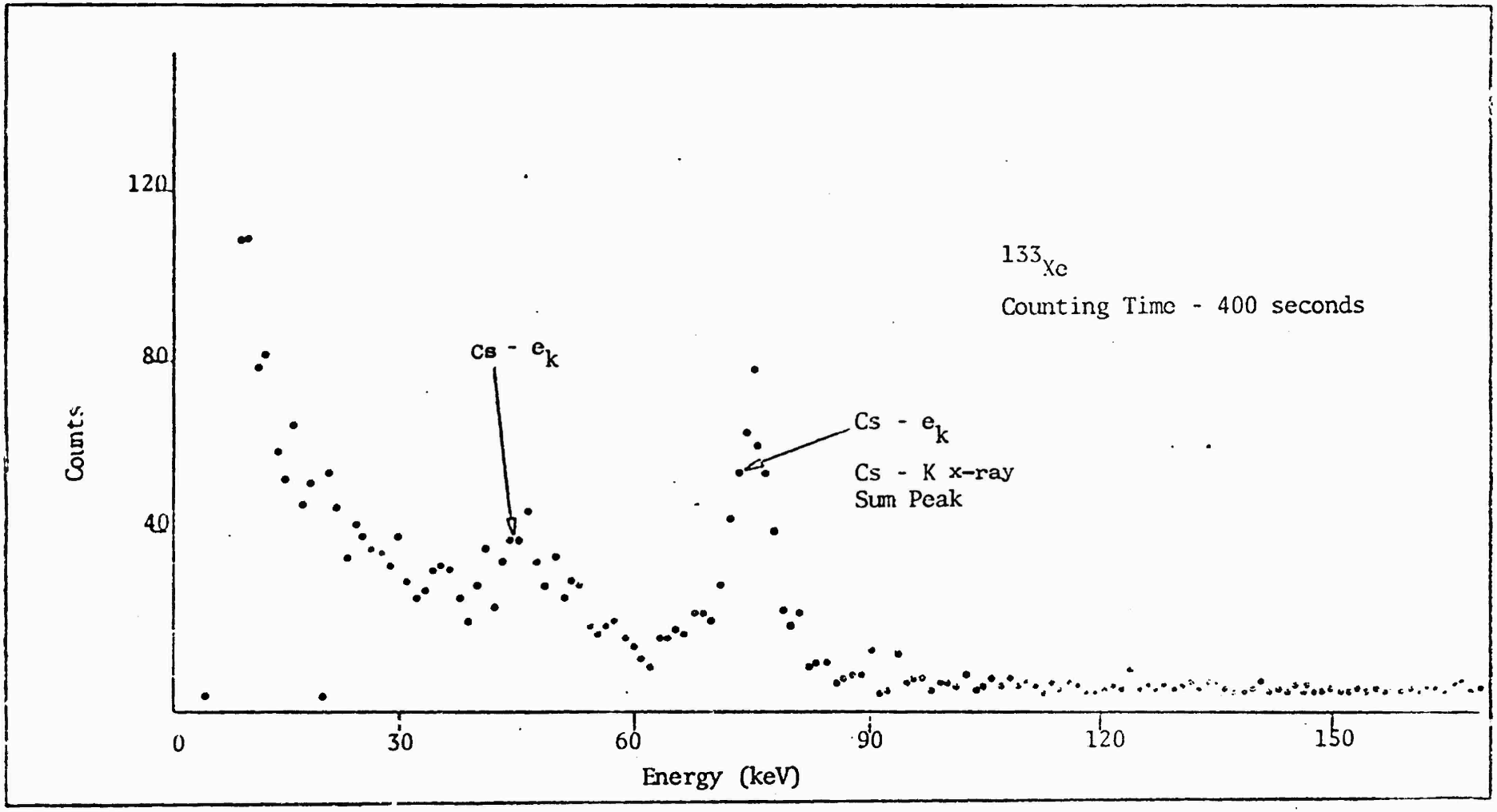

Figure 21. Xenon-133 Conversion Electron Spectrum

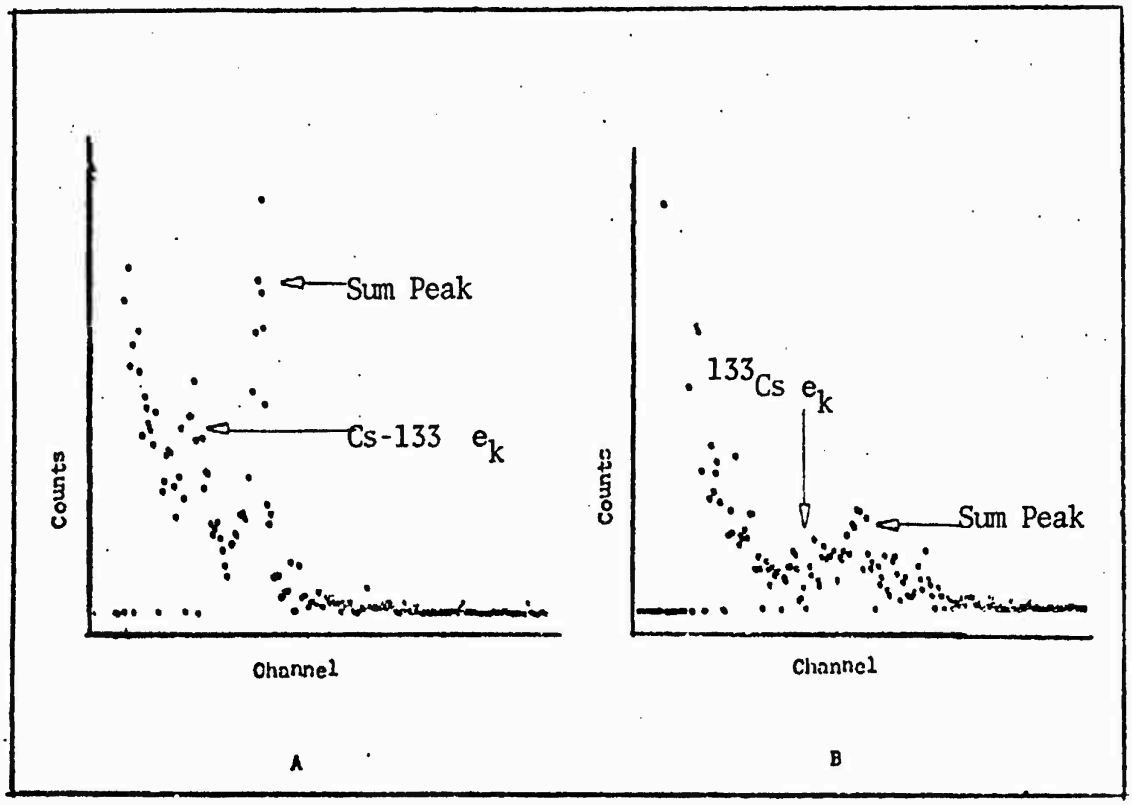

Figure 22. Effects of Impurities on the ^{133}Xe Spectrum

energy resolution. The purity of the gas can be monitored by watching the height of the pulse. Since oxygen has a very high coefficient of electron attachment, the pulse height is also sharply decreased by oxygen (or air) contamination.

The earlier operation of the detector with P-10 counting gas at both atmospheric and high pressure is shown in Figures 23, 24, and 25; external gamma sources were used. The P-10 gas was not purified for either atmospheric or high pressure counting, thus causing a decrease in spectral resolution. Results in this study concerning the predicted decrease in resolution, and increase in background with pressure are inconclusive. Overall background and resolution dropped slightly at higher pressures. A proper investigation, however, of the effects of pressure, bias voltage, and quench gas on detector resolution could not be accomplished due to the limitations on the upper level of high voltage/gain (-8000V), and to an insufficient amount of time.

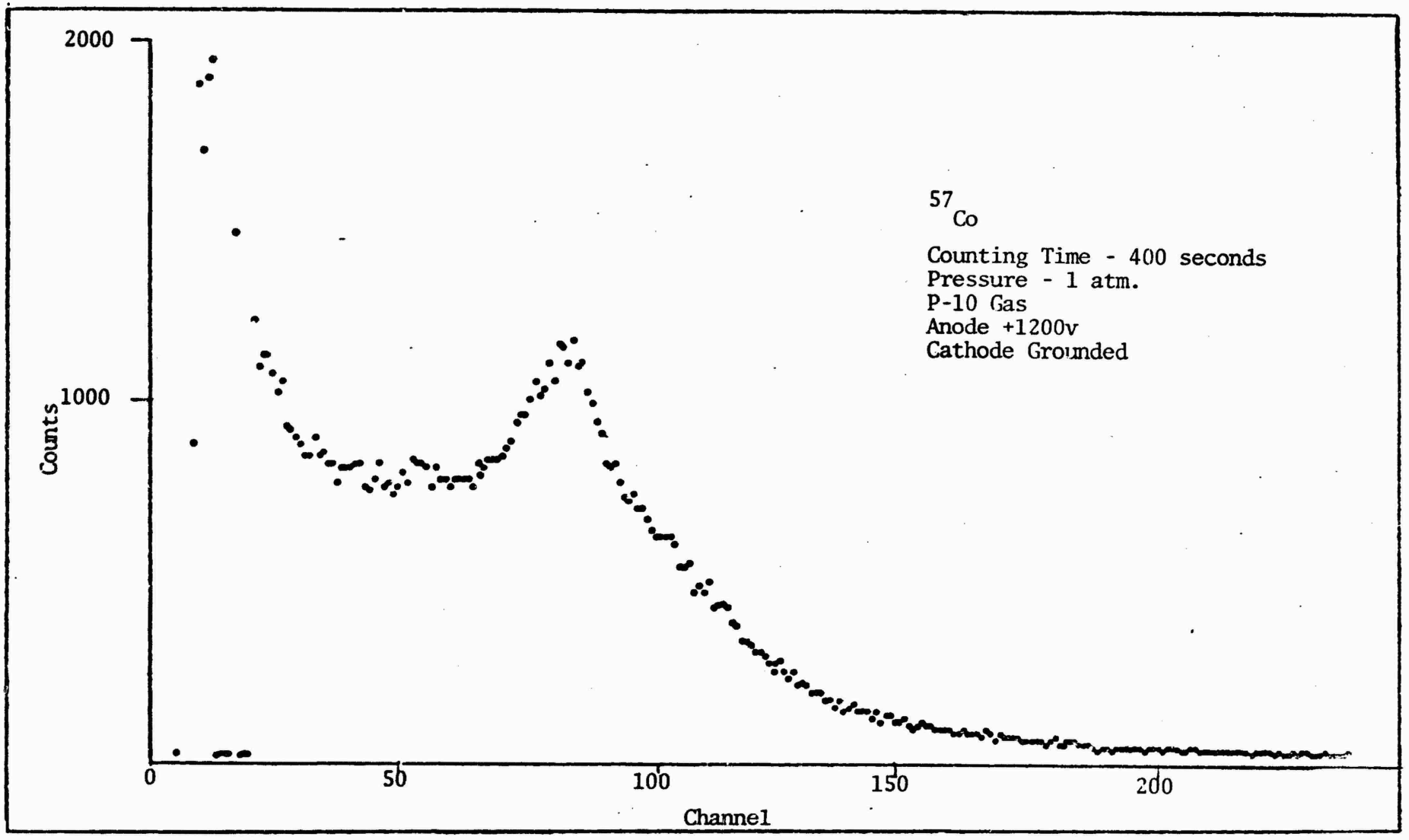

Figure 23. Cobalt-57 Gamma Ray Spectrum

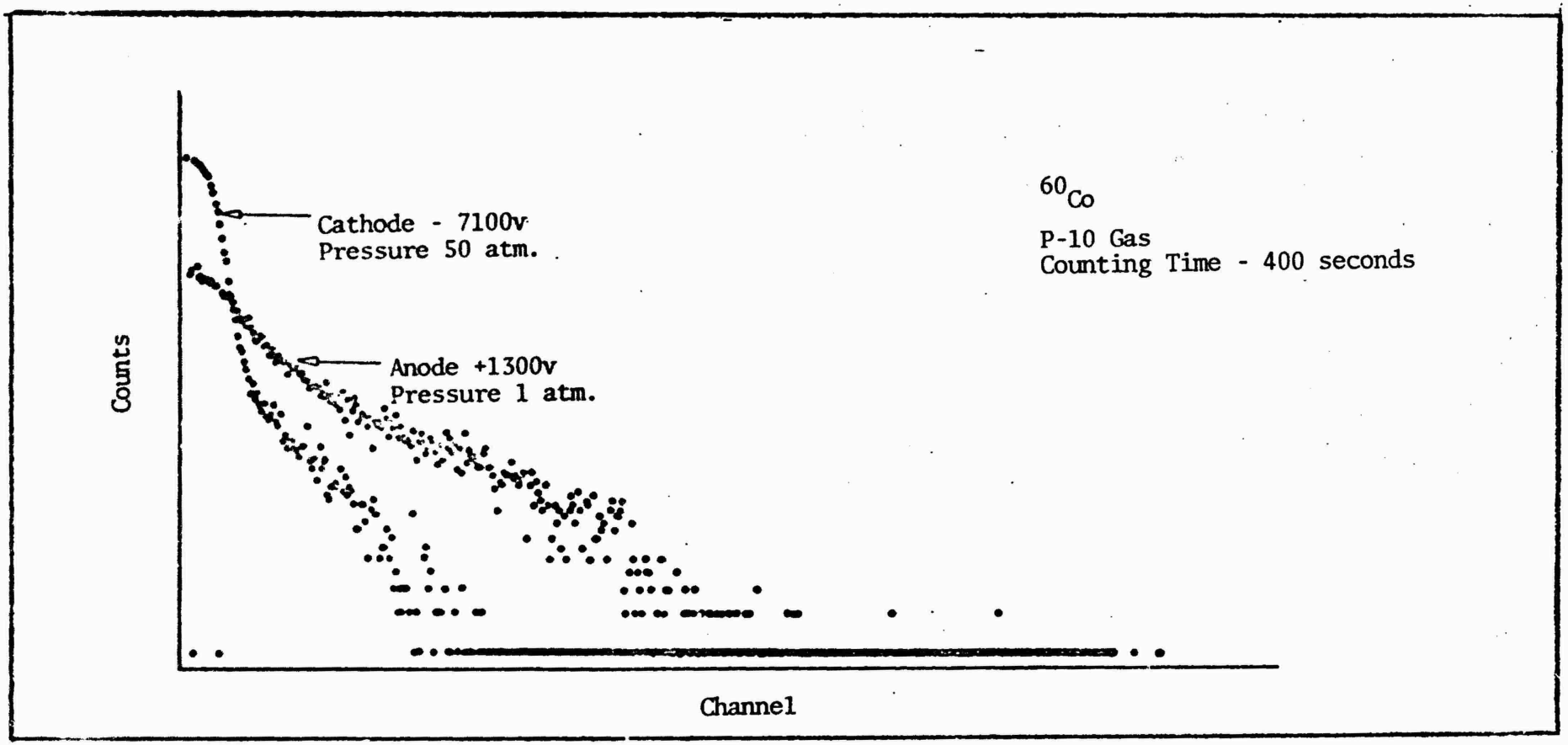

Figure 24. Cobalt-60 Gamma Energy Spectrum

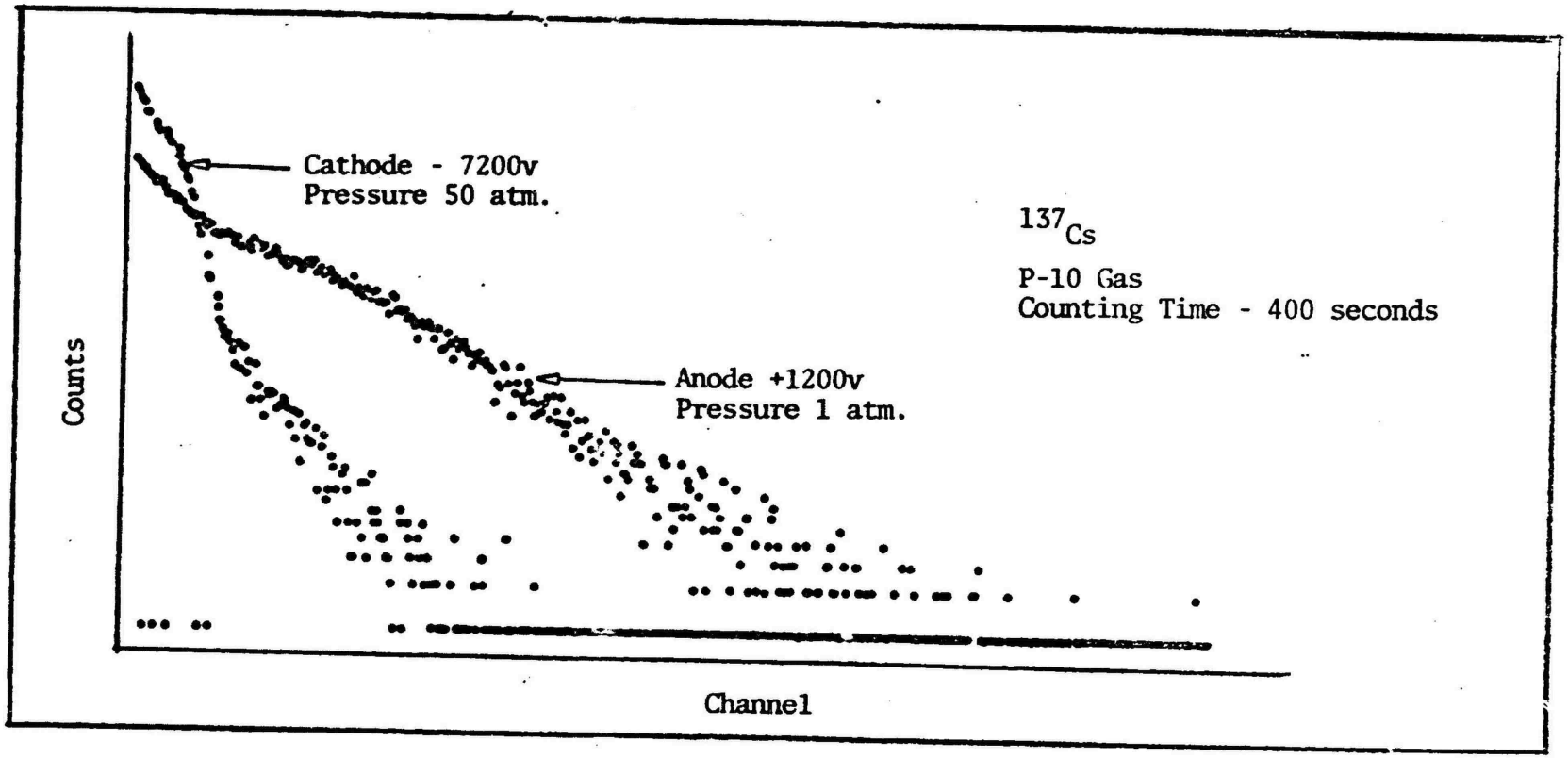

Figure 25. Cesium-137 Gamma Energy Spectrum

VI. Conclusions and Recommendations

Conclusions

On the basis of the results presented in the preceding chapter, the following conclusions can be drawn concerning the characteristics of the radiation detection system under study:

1. A high pressure xenon proportional counter may be used for the identification of the radionuclide ^{133}Xe by internal conversion electron analysis.

2. High pressure proportional counters and the noble gases are extremely sensitive to electronegative impurities; periodic purification is required.

Recommendations

Based on observations made during this project, the following recommendations are made for further study:

1. The electrical discharge from the cathode to the guard tube must be eliminated, and resolved by more efficient insulation or a design modification.

2. The characteristics of a high pressure proportional counter should be examined as the voltage, pressure, and quench gas are varied.

3. The capabilities of this system for determining a very small amount of ^{131m}Xe in the presence of ^{133}Xe should be investigated.

Bibliography

1. Currie, Lloyd. "The Measurement of Environmental Levels of Rare Gas Nuclides And The Treatment of Very Low-Level Counting Data," National Bureau of Standards, Washington, D.C., 1970.

2. Rowe, Charles E. Quantitative Analysis of Radioactive Noble Gases with a SiLi Detector. Unpublished thesis. Wright Patterson Air Force Base, Ohio: Air Force Institute of Technology, March 1974.

3. Hunt, K. K. Analysis of a Semiconductor Detection System for Measuring Radioactive Noble Gases. Unpublished thesis. Wright Patterson Air Force Base, Ohio: Air Force Institute of Technology, December 1976.

4. Andrews, Wayne L. Evaluation of a Detection System Employing Two Semiconductors for the Analysis of Radioactive Noble Gases. Unpublished thesis. Wright Patterson Air Force Base, Ohio: Air Force Institute of Technology, March 1982.

5. Berggren, Stephen R. A Cryogenic Argon Ionization Chamber Detector for Analysis of Radioactive Noble Gases. Unpublished thesis. Wright Patterson Air Force Base, Ohio: Air Force Institute of Technology, March 1982.

6. Beneddeti, Dale. A Cryogenic Xenon Ionization Chamber Detector for Analysis of Radioactive Noble Gases. Unpublished thesis. Wright Patterson Air Force Base, Ohio: Air Force Institute of Technology, March 1983.

7. Horrocks, D. L., et al., "Measurement of Radioactive Noble Gases by Liquid Scintillation Techniques," page 201 in Proceedings of the Noble Gas Symposium, ERDA CONF-730915, Stanley, R. E. and Moshissi, A. A., editors, 1974.

8. Knoll, Glenn F. Radiation Detection and Measurement. New York: John Wiley & Sons, 1979.

9. Legrand, J. et al. "High-Pressure 4 Proportional Counter for Internal Conversion Electron Measurements (^{139}Ce, ^{109}Cd, ^{99m}Tc)," Nuclear Instruments and Methods, 112: 101-102 (1973).

10. Lees, A. P. "Pressurized Proportional Counters for Coincidence Measurements," Nuclear Instruments and

Methods, Vol. 112: 95-99 (1973).

11. Schell, W. R. "An Internal Gas Proportional Counter for Measuring Low Level Environmental Radionuclides," Proceedings of the 155th meeting of the American Chemical Society. San Francisco, Ca., April 1968.

12. Batchelor, R. et al. "Helium-3 Filled Proportional Counter for Neutron Spectroscopy," The Review of Scientific Instruments, 26: 1037-1047 (November 1955).

13. Gilmer, T.E. et al. "High Pressure Proportional Counter," The Review of Scientific Instruments, Vol. 28: 634-635 (August, 1957).

14. Costa, E. et al. "High Pressure MWPC for Hard X-ray Astronomy," Nuclear Instruments and Methods, 156: 57-61 (1978).

15. Bamberger, A. "High Pressure Proportional Counters Operating in Pure Hydrogen". Nuclear Instruments and Methods, 156: 107-110 (1978).

16. Oeschger, H. and H. H. Loosli. "New Developments in Sampling and Low Level Counting of Natural Radioactivity". Proceedings of the International Conference on Low Level Radioactivity Measurements and Applications. High Tatras, Czechoslovakia, Bratislava (1979).

17. Clark, George L. and Gessner G. Hawley, Editors. The Encyclopedia of Chemistry. New York: Van Nostiand Rheinhold Company, 1966.

18. Walker, F. W. and G. J. Kirovac. "Chart of the Nuclides," Knolls Atomic Power Laboratory, Schenectady, New York, 1977.

19. Hampel, Clifford A., Editor. The Encyclopedia of the Chemical Elements. New York: Rheinhold Book Corporation, 1968.

20. Meek, M. E. and B. F. Rider. "Compilation of Fission Product Yields," Vallecitos Nuclear Center, ORNL-TM-3515, August, 1971.

21. Chitwood, R. B. "Production of Noble Gases by Nuclear Fission," page 76 in Proceedings of the Noble Gas Symposium, ERDA CONF-730915, Stanley, R. E. and Moghissi, A. A., Editors, 1974.

22. Schell, W. R. et al. "Electron Spectrometers for Xenon Radioisotopes," (Draft) National Bureau of Standards, U. S. Department of Commerce, Washington, D. C., 1982.

23. Lederer, C. M., et al. Table of Isotopes (Seventh Edition). New York: John Wiley & Sons, 1978.

24. NCRP Report #58. "A Handbook of Radiation Measurements and Procedures". National Council on Radiation Protection and Measurements. Washington, D. C. (1978).

25. Siegbahn, Kai. Alpha-, Beta-, and Gamma-Ray Spectroscopy. Volumes I and II. Amsterdam: North Holland Publishing Company, 1966.

26. Bambynek, W. "On Selected Problems in the Field of Proportional Counters," Nuclear Instruments & Methods, Vol. 112: 103-110 (1973).

27. Charles, M. W. "Gas Gain Measurements in Proportional Counters," Journal of Physics E: Scientific Instruments, Vol. 5: 95-100 (1972).

28. Rose, M. E. and S. A. Korff. "An Investigation of the Properties of Proportional Counters." Physical Review, Vol. 41: 850-859 (June 194?).

29. Curran, S. C. and J. D. Craggs. Counting Tubes. Academic Press, London 1949.

30. Williams, A. and R. I. Sara. "Parameters Affecting the Resolution of a Proportional Counter," International Journal of Applied Radiation and Isotopes, Vol. 13: 229-238 (1962).

31. Zastawny, A. "Gas Amplification in a Proportional Counter with Carbon Dioxide," Scientific Instruments, Vol. 43: 179-181 (1966).

32. Campion, P. J. "A Study of Proportional Counter Mechanisms," International Journal of Applied Radiation and Isotopes, Vol. 19:219-234 (1968).

33. Povinec, Pavel. "A Study of Proportional Counter Optimization for Long-Term Counting," Nuclear Instruments and Methods, Vol. 163: 363-368 (1979).

34. English, W. N. and G. C. Hanna. "Grid Ionization Chamber Measurements of Electron Drift Velocities In Gas Mixtures," Canadian Journal of Physics, Vol. 31: 768-797 (1953).

35. Bowe, J. C. "Drift Velocity of Electrons in Nitrogen, Helium, Neon, Argon, Kryton, and Xenon," Physical Review, Vol. 117: 1411-1415 (March 1960).

36. Spila, H. "Inert Gas Mixtures for Proportional Counters," Nuclear Instruments and Methods, Vol. 140: 389 (1977).

37. Pisarev, A. F. et al. "A New Particle Detector - The Crystal Filament Counter," Soviet Physics JETP, Vol. 36: 828-834 (May 1973).

38. Kubota, S. "Non-Metastable Penning Effect in the Alpha-Particle Ionization of Inert Gas Mixtures," Journal of the Physical Society of Japan, Vol. 29: 1017-1029 (October 1970).

39. Rossi, Bruno and Hans H. Staub. Ionization Chambers and Counters. New York: McGraw Hill Book Company, Inc., 1949.

40. Korff, Sage A. Electron and Neutron Counters. New York: D. Van Nostrand Company, 1955.

41. Cockroft, A. L. and S. C. Curran. "The Elimination of the End Effects in Counters," The Review of Scientific Instruments, Vol. 22: 37-42 (January 1951).

42. Riggs, F. B. "New Design for a Gas-Flow Proportional Counter," The Review of Scientific Instruments, Vol. 34: 392-395 (April 1963).

43. Garfinkel, S. B. et al. "Present Status in the Field of Internal Gas Counting," Nuclear Instruments and Methods, Vol. 112: 59-67 (1973).

44. Horstman, H. M. et al. "Field Corrector for Proportional Counters," Nuclear Instruments and Methods, Vol. 112: 619-620 (1973).

45. Hendricks, R. W. "The Gas Amplification Factor in Xenon Filled Proportional Counters," Nuclear Instruments and Methods, Vol. 102: 309-312 (1972).

46. Charles, M. W. and B. A. Cooke. "Proportional Counter Resolution," Nuclear Instruments and Methods, Vol. 61: 31-36 (1968).

47. Fano, V. "Ionization Yield of Radiations. II. The Fluctuations of the Number of Ions," Physical Review, Vol. 72: 26-29 (July 1947).

48. Sipila, H. "Energy Resolution of the Proportional Counter," Nuclear Instruments and Methods, Vol. 133: 251-252 (1976).

49. Alkhazov, G. D. et al. "Ionization Fluctuations and Resolution of Ionization Chambers and Semiconductor

Detectors," Nuclear Instruments and Methods, Vol. 48: 1-12 (1967).

50. Alkhazov, G. D. "Mean Value and Variance of Gas Amplification in Proportional Counters," Nuclear Instruments and Methods, Vol. 75: 161-162 (1969).

51. Alkhazov, G. D. "Statistics of Electron Avalanches and Ultimate Resolution of Proportional Counters," Nuclear Instruments and Methods, Vol. 89: 155-165 (1970).

52. Campion, P. J. "Spurious Pulses in Proportional Counter," Nuclear Instruments and Methods, Vol. 112: 75-81 (1973).

53. Genz, H. et al. "Measurement by Two-dimensional Pulse Analysis of the Time and Energy Distributions of Afterpulses in Proportional Counters," Nuclear Instruments and Methods, Vol. 60: 195-200 (1968).

54. Ricker, G. R. and J. J. Groves. "Pulse Rise-times in Proportional Counters," Review of Scientific Instruments, Vol. 40: 227-233 (February 1969).

55. Gott, R. and M. W. Charles. "Attenuation of Proportional Counter Pulses by Equal Integrating and Differentiating Time Constants," Nuclear Instruments and Methods, Vol. 72: 157-160 (1969).

56. Baumeister, Theodore and Lionel S. Marks, eds. Standard Handbook for Mechanical Engineers (Seventh Edition). New York: McGraw-Hill Book Company, 1967.

57. Gibbs, D. S. et al. "Purification of the Rare Gases," Industrial and Engineering Chemistry, Vol. 48: 289-296 (January 1956).

58. Hodgman, Charles D. Handbook of Chemistry and Physics. Cleveland, Ohio: Chemical Rubber Company, 1962.

59. Drever, R. W. P. et al. "A Proportional Counter System with Small Wall Effect," Nuclear Instruments, Vol. 1: 41-45 (1957).

Appendix A.

Description of the High Pressure Xenon Proportional Counting System

Introduction

The high pressure xenon proportional detection system uses xenon as a proportional counting medium to spectrographically analyze radiation sources. The detection system consists of the following components: a gas handling system, a detector, and electronics. The electronics are discussed thoroughly in Chapter IV, and will not be presented here.

Two detectors and a gas handling system were constructed. Figure 14 is a detailed drawing of the first detector. Figure 16 is a sketch of the second detector. Figure 15 shows the entire detection system including vacuum components. The system electronics are shown in Figure 20.

The gas handling system consists of a gas reservoir, a breakseal tube, two cold fingers, a purifier, high pressure and vacuum valves, and associated components. The gas reservoir is a stainless steel cylinder, 15 inches long and 8.31 inches I.D., which has three 1/4 inch tube ports for swage-lok fittings to Nupro valves, and a 1/2 inch port with a soft-solder connection to a vacuum valve. A 3/8 inch O.D. tube port on top of the reservoir threads into a 25

P.S.I.D. capacity pressure transducer. The reference side of the gauge is connected via 7/8 inch I.D. copper tubing directly into the vacuum system. Nupro valves (#1 and #2) are connected through polypropylene tubing to high purity counting gases. All fittings are swage-loks, and a pressure regulator controls pressure in the line. Valve #3 and the vacuum valve are used to isolate the gas reservoir from the rest of the system. The vacuum valve is attached to a vacuum system consisting of a mechanical pump and a diffusion pump. The pump system is utilized to evacuate the system and to provide the reference vacuum for the pressure transducer.

Between valves #3-#5 is a 1/4 inch O.D. stainless steel "T" connection. Valve #5 is connected to a stainless steel holder for the breakseal tube via swage-lok fittings; the tube is firmly positioned in the holder by an o-ring. The breakseal tube introduces measured amounts of radioactive gas into the system for analysis. The first cold finger (L) is a capped stainless steel cylinder which is 5.25 inches long, 5/8 inch O.D., and silver soldered at a 90 degree angle to a 3.25 inches long tube of similar diameter. The counting gas an sample is cryogenically pumped through the detection system.. Valve #4 is connected to the cold finger by a swage-lok fitting to a 1/4 inch port. The other port is a 3/4 inch copper gasket flange which connects via a glass-to-metal seal to the purifier. The purifier is a 3/4 inch diameter quartz glass tube filled with zirconium and titanium turnings. The turnings are held in the tube by copper wool. Around the tube is

a double element cylindrical electric furnance encased in fire brick insulation. The furnance can easily heat the turnings to 1000°C. Graded bands on either side of the purifier protect the rest of the glassware from thermal stress.

The purifier is connected by another 3/4 inch copper gasket flange port to a 1/4 inch O.D. stainless steel bellows, and via a swage-lok fitting to Nupro valve #6. The steel bellows prevents excessive torque on the purifier. The "T" connection between valves #6-#8 consists of stainless steel tubing with swage-lok fittings for the valves, another bellows, and a 1/4 inch I.D. glass insulator bounded with glass-to-metal seals. The glass insulator protects the gas handling system from the high voltage present in the detection section during operation. Valve #7 connects to a stainless steel fitting which screws onto a 1/2 inch O.D. drierite container, utilized for the purification of CO_2 quench gas. Finally valve #8 is connected by another 3/4 inch copper gasket flange port to a 0.37 inch I.D. tube which is welded at a right angle to a 8.25 inches long cold finger (E) of similar diameter. The second detector has a cold finger of length 14 inches.

First Detector

The cold finger is threaded into a 1/2 inch gas inlet in the counter wall, and silver soldered inside and outside of the detector. The counter body was machined from stainless steel 303. The detector is 5.25 inches long, 0.20 inch thick, 1.61 inches I.D., and 2.0 inches O.D. The 0.058 inch

O.D. anode wire support tube has a 1/4 inch boss on one end which is seated and epoxyed inside the guard tube well on a 0.3 inch O.D. quartz insulator. The quartz insulator is itself epoxyed against the inside base of the guard tube electrode. The guard tubes, with length 0.375 inch and 0.187 inch O.D., are at ground potential and function as insulators for the central wire. The guard tubes are composed of two separate components. The guard tubes widen to 0.56 inch O.D. threaded connectors which screw onto the guard tube electrodes; the electrodes pass through the endplates for external electrical connections. The outside base of the guard tube electrodes are epoxyed to 1/8 inch wide, 0.6 inch O.D. quartz insulators. The insulators are epoxyed to the inside of the field tube electrodes.

The field tubes prevent distortion of the electric field from end effects. The field tubes, with length 0.56 inch and 0.38 inch O.D., operate at high negative bias. The outside base of the field tube electrodes are epoxyed to 1/4 inch wide, 0.74 inch O.D. quartz insulators; the insulators are epoxyed to a circular step in the endplates.

The end of the detector is fitted with electrically screened brass covers with a plexiglass endplate. A low voltage connector is centered in the plexiglass endplate; it electrically connects the brass anode wire connection (Chapter V) to the preamplifier, and is also modified to slip over the exterior guard tube electrode. A concentric phenolic insulator is wrapped around the connector; a concentric brass

cylinder is clamped on the phenolic, and fitted over the field tube electrode. An RG 8/U cable from the high voltage power supply is soldered to the brass cylinder. A brass plug, silver soldered to the exterior of the cathode, serves as the electrical connection for the high voltage supply. A 1/2 inch thick protective lucite shield covers the first detector, cold finger, and high pressure valve.

Second Detector

The second detector is machined from stainless steel 304. The counter is 5.25 inches in length, 1.62 inches I.D., 3.0 inches O.D., and 0.69 inches thick. The endplates are fastened to the counter with six 1/4 inch screws, and sealed with a soft copper ring between two knife edges. The field tubes are 0.81 inch long, 0.30 inch I.D., and widen at the bottom into 0.4 inch long, 0.75 inch I.D. cups which are epoxyed to a circular shelf on the plexiglass insulators. The guard tubes are 0.5 inches long, and 0.5 inches I.D.; they are set against 1/8 inch wide, 0.75 inch O.D. collars which surround 1 inch, 0.25 inch O.D. guard tube electrodes.

There are three plexiglass insulators. The first insulator cups the 1/8 inch boss on the anode wire support tube. The boss is epoxyed to the plexiglass insulator, and the insulator is epoxyed to the guard tube and collar. The second insulator is the seat for all end pieces, and is epoxyed to a circular step in the endplate. The third insulator protects the electrical connection screw for the field [illegible]

bonded to the endplate.

The anode wire support tube is 3 inches in length with a 1/8 inch O.D., 3/16 inch long boss in the center. The high voltage connection to the field tube is through a #5 brass screw. A brass collar with a lip attachment presses firmly against the field tube. The high voltage cables, RG 8/U, are bolted to the screws from the outside. Low voltage connectors are utilized for the guard tube electrodes, and anode wire electrical connection. A brass plug connector is screwed into the cathode body for the high voltage supply cable.

Appendix B

Operating Procedures for the High Pressure Xenon Proportional Counter

The two proportional counters are operated in much the same manner. Each stage of operation is described below. The components and valves are identified in Figure 15. The diffusion pump by-pass valves and the diffusion pump vacuum valve are not shown.

Purging

1. Close the diffusion pump by-pass valve (X). Open by-pass valve (Y). Close the diffusion pump vacuum valve (Z). Close the gas reservoir vacuum valve.

2. Open valve #2 (argon valve) and pressurize the system to about 20 Pace units (PU).

3. Close the argon valve and open the vacuum valve. Pump until the pressure is less than about 10 microns.

4. Close the gas reservoir vacuum valve.

5. Repeat 2 through 4 as often as desired.

Cleaning

1. Open all valves except #1, #2, #5, and #7.

2. Open the vacuum valve. Pump until the pressure is at the lowest possible range (ideally 10^{-7}torr). The purifier should be operating at greater than 700°C. This procedure is

utilized only with the diffusion pump and mechanical pump operating. To clean only with the mechanical pump, the diffusion pump by-pass valve (X) near the mechanical pump should be closed, and the by-pass valve (Y) near the gas reservoir opened. The diffusion vacuum valve (Z) should also be closed.

3. Close all valves.

Introducing the Sample

1. Put the sample breakseal tube into the breakseal connector.

2. Close diffusion pump by-pass valve X, open by-pass valve Y. Close the diffusion pump vacuum valve Z. Open valve #5 (breakseal valve). Pump until the pressure is less than 10 microns.

3. Open by-pass valve X, close by-pass valve Y. Open the diffusion pump vacuum valve Z. Pump to the desired pressure.

4. Close valve #5. Break the breakseal tip.

Introducing the Xenon

1. Introduce the sample as described above.

2. Close the gas reservoir vacuum valve. Isolate the gas reservoir by closing valve #3.

3. Open valve #1 and introduce one atmosphere of xenon into the gas reservoir.

4. Close the xenon valve and open valve #3 slowly.

5. Cool the breakseal tube with liquid nitrogen (LN).

6. After the sample in the breakseal tube is condensed, cool the first cold finger with LN.

7. Open valve #5.

Purifying the Xenon Sample

1. Make sure the purifier is at 1000° C.

2. Cool the detector cold finger with LN. Allow the first cold finger to warm.

3. Cool the first cold finger with LN. Allow the detector cold finger to warm.

4. Repeat 2 and 3 as often as needed to reach the desired purity. Once the desired purity is reached, stop the process at 2.

Pressurizing the Counter

1. When the vapor pressure of xenon is at LN temperature, zero Pace units, close valve #8.

2. Let the cold finger warm to room temperature.

3. Slowly open the gas reservoir vacuum valve after bypassing the diffusion pump.

Spectrum Collection

1. Turn on preamplifier, amplifier, high voltage power supplies, oscilloscope, multichannel analyzer, timer/scaler, and single channel analyzer.

2. Slowly apply negative biasing voltage to the detector while observing the output of the preamplifier on the oscilloscope. Slowly approach the cathode voltage predicted for the multiplication desired using the Diethorn equation or from experiment. Watch for high voltage breakdown.

3. Adjust the gain of the amplifier while observing the output of the amplifier on the oscilloscope.

4. Set the desired collection time on the multichannel analyzer and begin spectrum collection.

Vita

PII Redacted

Jeffrey Joseph Knapp [redacted] [redacted] [redacted] the son of Bernard R. Knapp and Blanche Knapp. After graduating from Glenwood High School he was accepted for enrollment at the United States Military Academy in West Point, New York. He graduated in 1974 and was commissioned a lieutenant in the U.S. Army. He next attended Airborne School at Fort Benning, Georgia, followed by the Air Defense Officer's Basic Course and the Nike Hercules Weapon's Option at Fort Bliss, Texas. He spent six years in Hardheim, Germany, as a launcher platoon leader, executive officer, and commander of a Nike Hercules Missile Firing Battery. While in Germany he enrolled in the University of Southern California, graduating in 1978 with a Master of Science in Systems Management degree. After leaving Germany, he completed the Air Defense Officer's Advanced Course at Fort Bliss, Texas, and was subsequently assigned to the Air Force Institute of Technology in 1981.

[redacted] [redacted]

This thesis was typed by Ruth E. Walker, Circle Computing, Inc.

PII Redacted

REPORT DOCUMENTATION PAGE

READ INSTRUCTIONS BEFORE COMPLETING FORM

1. REPORT NUMBER: AFIT/GNE/83M-8	2. GOVT ACCESSION NO.: AD-A135803
3. RECIPIENT'S CATALOG NUMBER:	
4. TITLE (and Subtitle): STUDY OF THE CHARACTERISTICS OF HIGH PRESSURE PROPORTIONAL COUNTERS FOR THE DETECTION OF NOBLE GASES.	5. TYPE OF REPORT & PERIOD COVERED: MS Thesis
	6. PERFORMING ORG. REPORT NUMBER:
7. AUTHOR(s): Jeffrey J. Knapp, CPT, USA	8. CONTRACT OR GRANT NUMBER(s):
9. PERFORMING ORGANIZATION NAME AND ADDRESS: Air Force Institute of Technology (AFIT-EN), Wright-Patterson AFB, Ohio 45433	10. PROGRAM ELEMENT, PROJECT, TASK AREA & WORK UNIT NUMBERS:
11. CONTROLLING OFFICE NAME AND ADDRESS:	12. REPORT DATE: March 1983
	13. NUMBER OF PAGES: 104
14. MONITORING AGENCY NAME & ADDRESS(if different from Controlling Office):	15. SECURITY CLASS. (of this report): Unclassified
	15a. DECLASSIFICATION/DOWNGRADING SCHEDULE:

16. DISTRIBUTION STATEMENT (of this Report)

Approved for public release; distribution unlimited.

17. DISTRIBUTION STATEMENT (of the abstract entered in Block 20, if different from Report)

18. SUPPLEMENTARY NOTES

Approved for public release: IAW AFR 190-17.
LYNN E. WOLAVER
Dean for Research and Professional Development
Air Force Institute of Technology (AIC)
Wright-Patterson AFB OH 45433
9 SEP 1983

19. KEY WORDS (Continue on reverse side if necessary and identify by block number)

Radioactive Noble Gases
Xenon
High Pressure Proportional Counter
Detection System

20. ABSTRACT (Continue on reverse side if necessary and identify by block number)

A system incorporating a high pressure proportional counter is examined for possible use in the quantitative analysis of radioactive noble gases. The analysis was limited to those radioisotopes of xenon, Xe-131m and Xe-133, which are produced in nuclear fission. The detector may be utilized for the identification of the radionuclide Xe-133 through conversion electron analysis. A sample of Xe-133 was measured at 41 atmospheres using xenon as the counting gas; the resolutions (FWHM)

for the 45 keV conversion electron and the 75.6 keV sum peak were found to be 5.9 keV and 7.0 keV respectively. The extreme sensitivity of noble gases to electronegative impurities was also found; a periodic purification may be required for stable and reproducible resolution.